Biomimetic Hydrogel-Based Actuating Systems

*Leonid Ionov**

Active motion is intrinsic to all kinds of living organisms from unicellular ones to humans and inspires development of synthetic actively moving materials. Hydrogels, which are three dimensional polymer networks imbibed with aqueous solutions, mimic the swelling/shrinking behavior of plant cells and produce macroscopic actuation upon swelling and shrinking. This Feature Article covers basic principles of design as well as recent advances in the development of hydrogel based actuating systems. It is discussed how simply swelling can be used to generate very complex multistep motion, which can be used to develop new optical devices, sensors, biomaterials, smart surface, etc.

1. Introduction

Active motion is intrinsic to all kinds of living organisms from unicellular ones to humans. In nature motion occurs on every scale of organization of organisms: from individual animals or their groups down to a single molecule. For example, motor proteins convert chemical energy directly into mechanical work and allow cell migration, division, sensing and adaptation.[1] Contrary to animals, where macroscopic movement is provided by cooperative nanoscale movement of motor proteins,[1a] motion in plants is provided by microscopic swelling of cells[2] (**Figure 1**a). In different schemes relatively slow swelling/shrinking can result in slow shape changes such as elongation, contraction, bending, twisting or fast snap-buckling and fracture-dominated movement that allow their rotation toward the sun, growth and dissemination of seeds.[2,3] Nature has many actuators, such as jellyfish, sea cucumbers, sea anemones, Venus flytraps, touch-me-nots, etc.

Hydrogels, which are three dimensional polymer networks imbibed with aqueous solutions, mimic the swelling/shrinking behavior of plant cells and produce macroscopic actuation upon swelling and shrinking (Figure 1b).[4] There are also many reports describing the design of hydrogels, which can swell and shrink in response to a change in light intensity, pH, temperature, biochemical processes, and electric and magnetic fields.[5] Exposure to one or multiple stimuli causes reversible contraction/swelling of hydrogels that is due to a change of interactions of the polymer molecules with water. The reversible changes in size and shape of hydrogels have found broad applications in the design of micromechanical and drug delivery systems, as well as for microfluidic devices and sensors (see recent reviews).[4b,6]

In the first part of the Feature Article (Section 2), a brief description of reversible mechanisms of movement in plants is given. Design and applications of hydrogel actuators based on principles of movement in plants and other more complex mechanisms of movement is discussed in the second part (Section 3).

2. Reversible Movement of Plants

This section aims to give brief overview of mechanism of reversible movement in plants. The more detailed overviews of different mechanisms of movement of plants are given in recent reviews.[2,3,8] The irreversible movement due to growth of cells and disruption of tissues is not discussed.

Uptake and release of water is the main driving force of movement in plants. One aspect of this phenomenon is turgor pressure caused by osmotic flow of water in cells, which is due to concentration gradients (**Figure 2**a). In many cases, a whole organ is actuated by the changes in turgor pressure. Two prominent examples of rapid movements are the leaf folding of mimosa (*Mimosa pudica*) and of the Venus flytrap (*Dionaea muscipula*). Another aspect of swelling-driven deformation of plant tissues is swelling and shrinking of cell walls (Figure 2b). In this case, the directionality of deformation is controlled by orientation of cellulose fibers. The principle is based on the fact that the length of cellulose fibrils remains unchanged and swelling occurs preferentially in the direction perpendicular to the fibrils. A well-known example is the release of ripe seeds from conifer cones. The cones are formed by two kinds of tissues with different orientation of cellulose fibrils. As a result, length of one kind of the tissue and the width of another one increases in humid environments. This inhomogeneous increase in the volume results in opening of the cone.[9]

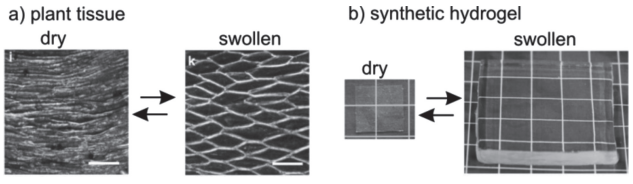

Figure 1. a) Reversible swelling of natural plant tissue of ice plant seed capsules. Reproduced with permission.[2a] Copyright 2011, Nature Publishing Group. b) Synthetic polymer hydrogel. Reproduced with permission.[7] Copyright 2011, American Chemical Society.

Dr. L. Ionov
Leibniz Institute of Polymer Research Dresden
Hohe Str. 6, D-01069 Dresden, Germany
E-mail: ionov@ipfdd.de

DOI: 10.1002/adfm.201203692

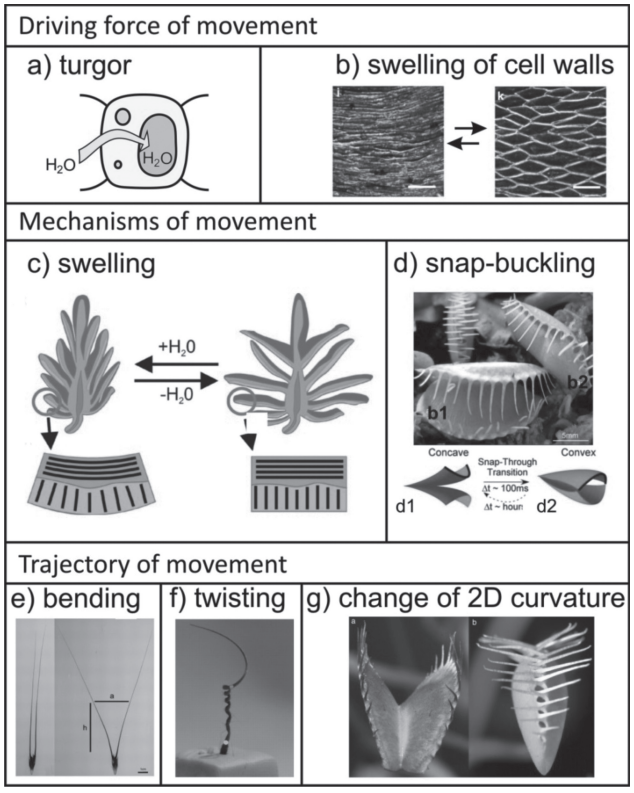

Figure 2. Summary of examples of reversible movement in plants with respect to driving force: a) turgor, b) swelling of cell walls; mechanism: c) swelling, d) snap-buckling; and trajectory: e) bending, f) twisting, g) change of 2D curvature of movement. b) Reproduced with permission.[2a] Coypright 2011, Nature Publishing Group; c) Reproduced with permission.[13] Copyright 2011, Elsevier; d) Reproduced with permission.[14] Copyright 2007, Wiley-VCH; e) Reproduced with permission.[3b] Copyright 2007, AAAS; f) Reproduced with permission.[12] Copyright 2011, The Company of Biologists Ltd; g) Reproduced with permission.[15] Copyright 2012, Elsevier.

It was observed that a change in the amount of water in plant tissues can result in relatively slow movement, such as in the case of cone, or can lead to extremely fast movement, such as in the case of Venus flytrap. The origin of the difference in the speed of actuation is the mechanism of the movement.[8] In the case of the cone, tissues with different orientation of cellulose fibrils act as classical bilayers, as described by Timoshenko:[10] an increase of the volume of one of the components results in bending (Figure 2c).[9] The geometry of the Venus flytrap is far more complex. The leaf has a doubly curved shape and a bistable configuration. Swelling of the cells results in snap-buckling transition from one stable state to another (Figure 2d).[11]

It was found that change of the amount of water in plat tissues can results in various shape changes. Wheat awn and pine cone bend when humidity changes that is used for burying itself and dissemination of seeds, respectively (Figure 2e).[3b,9] The filaree (*Erodium cicutarium*) seeds can bury themselves by drilling into the ground, twisting and untwisting in response to changes in humidity (Figure 2f).[12] The Venus flytrap changes its shape from double curved to another one that is used to trap insects (Figure 2g).[11]

Leonid Ionov came to Leibniz Institute of Polymer Research Dresden in 2009 as a group leader for stimuli-responsive interactive polymeric materials. After studying polymer chemistry at the Lomonosov Moscow State University/ Russia and graduation at the Technical University Dresden he spent his post-doc at the Max Plank Institute of Molecular Cell and Biology with Prof. S. Diez, working on biomolecular motors on responsive thin polymer films. He completed a research stay at the Clarkson University/USA with Prof. S. Minko working on biotechnology approaches. 2012 he was awarded with the Georg Manecke Award of the GDCh (German Chemical Society). The research of Leonid Ionov is multi-disciplinary and exploratory positioned at the interface between synthetic polymer chemistry, physics and cell biology. His current focus lies on the design and self-assembly of functional stimuli-responsive polymeric materials and bio-active hydrogels.

3. Hydrogel-Based Moving Systems

This part of the article aims to discuss principles of design of actuating structures, based on reversible swelling/shrinking of stimuli-responsive hydrogels. Typically change of conditions such as temperature, pH, light, results in homogeneous expansion or contraction of hydrogels in all directions that is similar to swelling/shrinking of cells (**Figure 3**a). Complex deformation such as bending and twisting as well as even more complex folding is produced as a result of inhomogeneous expansion/ shrinking, which occurs with different magnitudes in different directions[16] and can be achieved either (i) by applying inhomogeneous field, for example gradient of temperature or concentration, to homogeneous materials (Figure 3b) or (ii) by applying homogeneous field to inhomogeneous materials (Figure 3c). There is no known example in the plants,

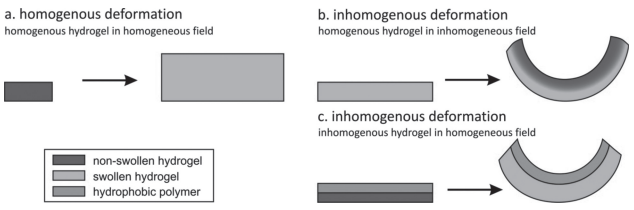

Figure 3. Different scenario of swelling of hydrogels: a) homogeneous deformation of homogeneous hydrogel; b) inhomogeneous deformation of homogeneous hydrogel; c) inhomogeneous deformation of inhomogeneous hydroge

where applying an inhomogeneous field to homogeneous materials (Figure 3b) was used, because it is rather difficult to keep the concentration or temperature gradient constant. Nevertheless, this approach is included in the present article, since it is very important part of the field of hydrogel-based actuators. The plants typically form tissues with inhomogeneous properties (Figure 3c), which are use used to produce complex movements such as bending or twisting.

3.1. Homogeneous Deformation of Hydrogels

3.1.1. Microgels

In most cases swelling/shrinking results in a change of volume of the hydrogel object while the shape remains nearly the same; this is similar to the behavior of plant cells.[17] Homogenous swelling, for example, is demonstrated by thermoresponsive poly(N-isopropylacrylamide)-based hydrogel micro- and nanoparticles. The microgel particles swell above the lower critical solution temperature (LCST) and shrink below the LCST. Homogeneous swelling of hydrogel microparticles can be used for a variety of applications. For example, reversible swelling and shrinking of thermoresponsive and pH-sensitive hydrogels was used as a mean for smart release of drugs.[18] The microgel particles, which have transition temperature of around 40 °C, are imbibed with water-soluble drug. The microgel particles are swollen at normal body temperature and the drug is not released. Since the inflammation induces a local increase in temperature, the drug-loaded microgel particles shrink at the point of inflammation which leads to the release of drugs.[19] Stimuli-responsive hydrogel microparticles can also be used as microlenses with tunable by external stimuli focal length.[20] Incorporation of gold or semiconductor nanoparticles in hydrogel particles, which are able to reversibly change their volume, can be used for design of hydrogel-based materials with tunable optical properties.[21] In this case, swelling and shrinking of hydrogel particles results in the change of aggregation/disaggregation of the incorporated nanoparticles that change their plasma resonance properties or fluorescence. Closely-packed homogeneous swelling hydrogel microparticles can also be used for design of photonic crystals with switchable optical properties.[22] Spherical particles form densely packed arrays, their periodicity being defined by the size of the particles and their reversible swelling/shrinking being responsible for changes in the periodicity of the lattice that results in the change of the wavelength of transmitted and reflected light. Different signals, such as mechanical treatment,[23] temperature,[22d] light, magnetic[24] and electric[25] fields were used as stimuli to switch optical properties. Notably, this mechanism of switching of periodicity is similar to the natural mechanism of the change in coloration of squid.[1e]

3.1.2. Macroscopic Hydrogels

Large pieces of hydrogels demonstrate similar homogeneous swelling;[17a] the size of sample changes while the shape remains unchanged. The homogeneous swelling/shrinking of macroscopic hydrogels was used to control the flow inside microfluidic devices.[26] The hydrogel acts as a smart valve, which allows the liquid to flow when the hydrogel is shrunk and closes the channel when swollen. There are many examples of such smart microfluidic valves sensitive to various signals, such as pH, temperature, enzyme, light and electric field.[27] For lab-on-a-chip applications, the use of light and electric field as stimuli hold the promise, since they allow switching with both high spatial and temporal resolution. For example, Richter and co-workers explored possibilities to control the liquid flow by stimuli-responsive hydrogels. In particular, they used hydrogels as pumps and gates, which control liquid flow in microfluidic devices.[28]

Swelling/shrinking of hydrogels can be used not only to affect optical properties that are perceived by visual sense but also to change topography that can be felt by touching. Very recently, Richer and co-workers reported design of palpable displays based on thermoresponsive hydrogels.[29] They integrated 4000 temperature-sensitive controlled actuators, each of them being heated by an individual electro-heating element. The designed hydrogel array was able to form a visual and palpable artificial imaging system.

Homogeneous swelling of macroscopic layers was also applied for the design of sensors.[30] One approach is based on the direct detection of changes in the hydrogel volume or mass. This, for example, can be done by ellipsometry, quartz microbalance (for hydrogel thin films) or scattering techniques (for hydrogel particles).[30,31] Another approach for design of hydrogel-based sensors is the incorporation of semiconductor or metal nanoparticles into the hydrogel matrix. In this case, particles serve as optically active probes. Contraction/swelling of hydrogels switches interactions between nanoparticles that results in the change of optical properties[17a,32]

Macroscopic hydrogels have been utilized for design of smart lenses with switchable focal length as well. In particular, adjustment of focal length by changing the curvature of the meniscus between water and oil by switching of the swelling of hydrogel was used to tune focal length of the optical lens.[33] The basic design (**Figure 4**) consists of a stimuli-responsive hydrogel ring placed within a microfluidic channel system and sandwiched between a glass plate and an aperture slit, the latter with an opening centered over the ring. The microchannels are filled with water and oil is placed on top of this structure and capped with a glass cover slip. The sidewall and bottom surface of the aperture are hydrophilic and the top surface is hydrophobic, which ensures that the water–oil meniscus is pinned along the hydrophobic–hydrophilic contact line. When exposed to an appropriate stimulus, the hydrogel ring underneath the aperture responds by expanding or shrinking. This leads to a change in the volume of the water droplet located in the middle of the ring. The net volume change—the change in the volume enclosed by the ring and the change in water droplet volume—causes a change in the pressure difference across the water/oil interface that directly determines the geometry of the liquid meniscus.

Homogeneous swelling/shrinking of macroscopic hydrogels can be used to change the shape of mammalian cells. For example, Pelah and co-workers have developed an approach to

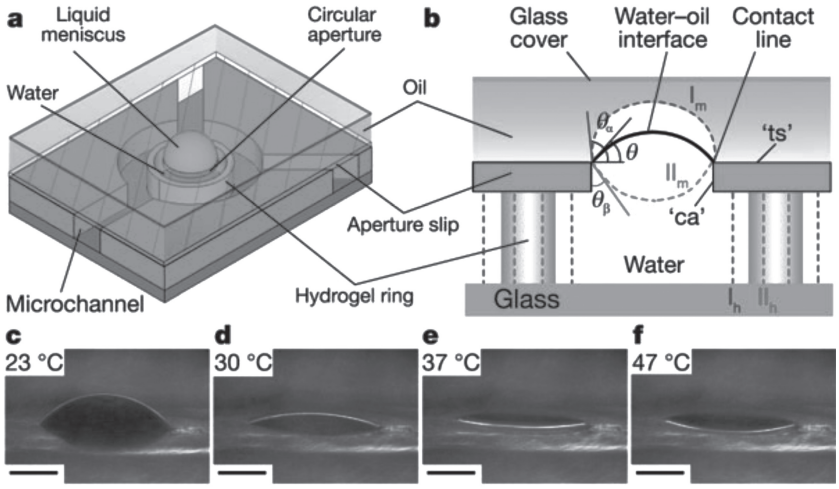

Figure 4. Design of smart lenses with switchable focal length using reversible swelling/shrinking of hydrogels. a) water/oil interface forms liquid microlens. Microchannels allow the flow of fluids to the microlens structure. b) Smart variable-focus mechanism. The hydrophilic sidewall and bottom surface ('ca') and hydrophobic top surface ('ts') of the aperture pin the water–oil meniscus along the contact line 'ca-ts'. The expansion and contraction of the hydrogel regulates the shape of the liquid meniscus by changing the angle θ of the pinned water/oil interface. The blue dashed lines show the expanded state of the hydrogel ring ('I_h') and the corresponding divergent microlens ('I_m') at $\theta = \theta a$. The red dashed lines show the contracted state of the hydrogel ring ('II_h') and the corresponding convergent microlens ('II_m') at $\theta = -(90° - \theta_\beta)$. c–f) The shape of the liquid microlens varies with local environmental temperature. Scale bars: 1.0 mm. Reproduced with permission.[33] Copyright 2006, Nature Publishing Group.

reversibly deform cells using a thermoresponsive polymeric actuator,[34] which squeezes the cell from two sides. Since the behavior of cells (differentiation, growth, apoptosis) depends on geometrical constraints, one can expect that this actuator can be used to study cell responses on mechanical treatment. Langer and Khademhosseini used a similar approach for the fabrication of 3D structures formed by two kinds of cells.[35] They fabricated thermoresponsive wells and filled them with cells at 24 °C when the hydrogel is swollen. The hydrogel was heated to 37 °C that caused its shrinking and formation of a gap between the cell cluster and the hydrogel well. The gap was filled with cells of a second kind. As a result, cell clusters with core formed by cells of one sort and shell formed by cells of a second sort were fabricated.

Very recently Aizenberg and Sidorenko demonstrated that homogeneous swelling of hydrogel films can lead to an "inhomogeneous" response and the appearance of anisotropic surface properties. They fabricated thin hydrogel films with incorporated high-aspect ratio rods. Collapse or swelling of the thin hydrogel layer caused change in the orientation of the rods[36] Due to the contraction of the polymer film upon drying, tensile forces arise, which are then transferred into a lateral actuation by nanocolumns, thus resulting in a tilt of the partially exposed nanostructures. The tilt angle is controlled by the volume change of the gel and can be therefore regulated by an appropriate choice of the polymer. Re-hydration of the sample leads to swelling and relaxation of the hydrogel. This results in normal orientation of the bristles (**Figure 5**).[37] These hydrogel films were, in particular, used for the design of surfaces with "conventional" and "reverse" switching behavior. These surfaces revealed conventional switching–hydrophilic after exposure to water and hydrophobic after drying if the rods are fixed on the surfaces. They could achieve reverse switching—hydrophobic after exposure to water and hydrophilic after drying—by using hydrogel films with non-fixed rods. The hydrogel-actuated hairs can further be used to control flow of reaction and to design really self-regulating systems. The idea is to fix a catalyst, which catalyzes certain chemical reactions, on the top of the hairs. Bending of the hairs changes the accessibility of the catalyst to the reagent in solution that affects the rate of chemical reactions. Use of thermoresponsive hydrogel coupled with the catalyst which catalyzes exothermic reaction allows for the design of self-regulating oscillating systems.[38]

Summary: The homogenous expansion/shrinking of hydrogels can be used for (i) controlled release of drugs, (ii) design of smart lenses with switchable focal length, (iii) design of materials with switchable coloration, (iv) control of flow in microfluidic devices, (v) design of sensors, (vi) control shape of cells and design complex 3D structures from cells, (vii) design of surfaces with switchable topography.

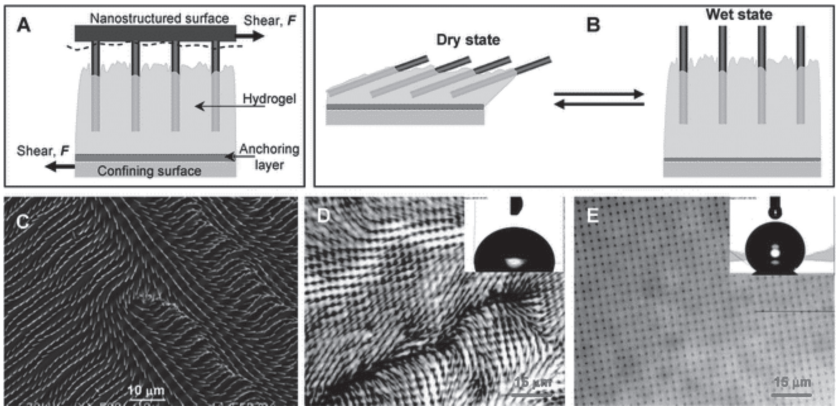

Figure 5. Gel-embedded array of rigid setae (GEARS) designed to provide a reverse response to exposure to water. a) Schematic of the setae transfer into the hydrogel layer attached to the confining solid surface modified with the PGMA anchoring layer upon in situ synthesis. b) Schematic illustration of the dynamic rearrangement of the GEARS in the dry and wet states. c) Representative SEM image of the GEARS bristle in the dry state. D) Optical microscopy analysis of the dry GEARS surface reveals highly tilted setae. The surface is relatively hydrophilic (d, inset). E) Optical microscopy analysis of the same region as in (D) in a humid atmosphere reveals setae standing perpendicular to the surface and its hydrophobic character (e, inset). Reproduced with permission.[37] Copyright 2008, Royal Society of Chemistry.

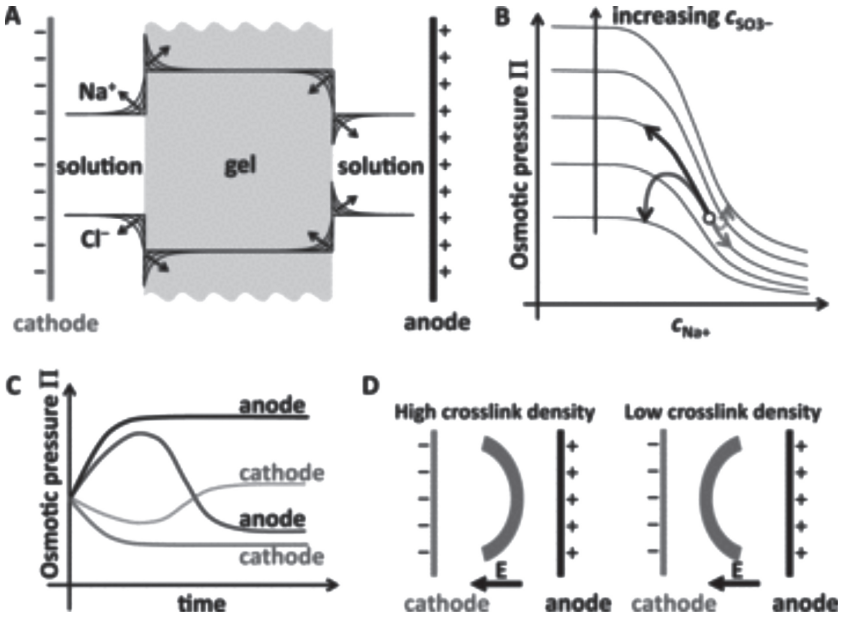

Figure 6. Theoretical concept behind unidirectional and bidirectional bending hydrogels. a) Expected accumulation of Na+ and depletion of Cl– ions at the cathode-side hydrogel boundary and depletion of Na+ and accumulation of Cl– ions at the anode-side hydrogel boundary with time. b) Variation of osmotic pressure with solution Na+ concentration for different concentrations of anionic groups (SO^{3-}) within the gel. Solid arrows indicate the anticipated (from Doi theory) monotonic swelling and shrinkage of a high crosslink density hydrogel at the anode (black) and cathode (gray) sides, respectively. Dashed arrows indicate the non-monotonic swelling behavior (from modification of Doi theory) expected from a low crosslink density hydrogel as a result of swelling and shrinkage of the gel causing large changes in the concentration of anionic groups within the gel. c) Time evolution of the osmotic pressure of a high and low crosslink hydrogels at the anode and cathode sides. Solid and dashed lines correspond to trajectories for high and low crosslink density hydrogels, respectively. d) Steady-state bent conformation of high and low-crosslink hydrogels predicted by our modified theory. Reproduced with permission.[46] Copyright 2011, Wiley-VCH.

3.2. Non-Homogeneous Deformation of Hydrogels

Non-homogeneous deformation (bending, twisting) could be achieved by applying either (i) an inhomogeneous field to homogeneous materials or (ii) homogeneous stimuli to inhomogeneous materials. An example of the first case is the bending of polyelectrolyte hydrogel in solution with lateral gradient of pH, which is formed during electrolysis[39] or PDMS strips with locally deposited solvent droplets.[40] Examples of the second group include bending of a liquid crystalline film,[41] hydrogel with a lateral gradient monomer concentration,[42] and cantilever sensors.[43]

3.2.1. Homogeneous Hydrogels in an Inhomogeneous Field

There are no known examples of the use this principle of movement in plants. The main reason is that it is rather difficult to generate and maintain continuous gradients (gradient of pH, salt concentration or temperature). On the other hand, this approach for the design of actuators is discussed in this paper since this is widely used for design of synthetic actuators.

It is well known that a strip of an anionic hydrogel bends towards the cathode in an electric field.[44] Doi and coworkers have provided a comprehensive theory to explain this behavior.[45] They predicted that the swelling behavior is governed by the concentration of the dominant ions and that the swelling speed is proportional to the square of the electric current.

Varghese and Arya have extended this theory in conceptual terms by relaxing one of its assumptions that the concentration of gel anionic groups remains constant during the bending process, which leads to a new scenario that the same anionic hydrogel can be made to bend in two different directions by changing its crosslink density.[46] They considered an anionic hydrogel poly (2-acryloylamido-2-methyl propane sulfonic acid) (PAMPS) containing SO_3^- within the electrolyte: NaCl solution. When an electric field is applied across the hydrogel, Na^+ and Cl^- ions travel towards the cathode and the anode, respectively. The Doi theory shows that with time the interfacial concentration of Na^+ will increase and decrease at the cathode and anode sides, respectively (**Figure 6**a). At the same time, the interfacial concentration of Cl^- will decrease and increase at the cathode and anode sides, respectively (Figure 6a). The theory also shows that for hydrogels with a fixed concentration of anionic groups (c_{SO3-}) that are fully dissociated, the osmotic pressure (Π) within the hydrogel decreases monotonically with increasing Na^+ concentration (c_{Na+}) on the solution side, and that each Π–c_{Na} plot (at fixed c_{SO3-}) shifts upward with increasing c_{SO3-} (Figure 6b). This implies that Π will increase at the anode side (due to decreasing c_{Na+}) and decrease at the cathode side (due to increasing c_{Na+}). The solid black and gray arrows in Figure 6b schematically depict one such trajectory of Π vs. c_{Na+} at the two hydrogel interfaces, and the solid black and gray lines in Figure 6c show the corresponding Π vs. time behavior. Thus, the model explains how anionic hydrogels swell at the anode side and shrink at the cathode side causing it to bend towards the cathode (Figure 6d left).

Varghese and Arya showed that an anionic hydrogel could be designed to swell on the cathode side and shrink at the anode side such that it bends towards the anode, exactly opposite to the behavior described by the Doi theory. Indeed, such a hydrogel could be achieved if one realizes that hydrogel swelling at the anode side is also accompanied by a decrease in the effective concentration of anionic groups (c_{SO3-}). Similarly, as the hydrogel shrinks at the cathode side, the effective concentration of anionic groups increases. This implies that the osmotic pressure trajectory at the anode side does not follow a single Π–c_{Na+} curve but instead moves downwards to lower Π–c_{Na+} curves corresponding to a smaller c_{SO3-} while climbing up each Π–c_{Na+} curve. Therefore, it is envisioned that if the change in c_{SO3-} is sufficiently large, the trajectory will exhibit a maximum in the Π–c_{Na+} plot and then dip downwards, as indicated by the black dashed arrow in Figure 6b and by the black dashed

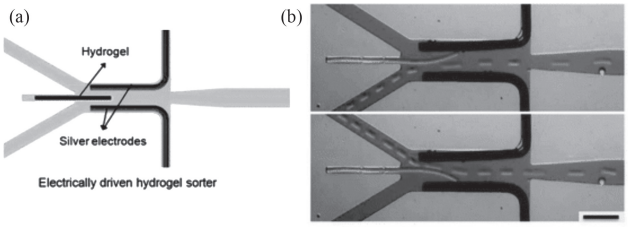

Figure 7. a) Schematic of the sorting device composed of three parts: an electrically-driven hydrogel sorter, a droplet generation channel, and a focused mEBs channel; b) Examples of droplet sorting (oil phase flow rate = 2 μL min^{-1} and water phase flow rate = 6 μL min^{-1}). The scale bar indicates 1 mm. Reproduced with permission.[39] Copyright 2010, Royal Society of Chemistry.

line in Figure 6c. At the cathode side, the osmotic pressure trajectory will hop to higher Π–c_{Na+} curves due to the increase in c_{SO3-} while climbing down each Π–c_{Na+} curve, allowing for the possibility of a reversal in the direction of Π, as indicated by the gray dashed arrow in Figure 5b and gray dashed line in Figure 6c. Depending on the conditions, the final location of the osmotic pressure at the anode side could end up lower than that at the cathode (Figure 6b,c), causing the gel to eventually bend towards the anode after transiently bending towards the cathode (Figure 6d, right).

Thus, it is expected lightly-crosslinked hydrogels to initially bend towards the cathode, then straighten out and eventually bend towards the anode (Figure 6d right). On the other hand, a highly crosslinked hydrogel that is relatively stiffer possesses little capacity to further swell or shrink in an electric field. The osmotic pressure of such a hydrogel would therefore be expected to exhibit the conventional monotonically increasing and decreasing osmotic pressure trajectory at the anode and cathode respectively, making the gel bend towards the cathode (Figure 6d left).

Bending of electroactive hydrogel strips in a microfluidic channel was applied to control flow as well as to sort particles and cells.[39] The hydrogel strip is integrated in a Y-junction and is able to bend either to one side or to another depending on the polarity of the applied voltage (**Figure 7**). It was demonstrated that the device is suitable for sorting mouse embryoid bodies (mEBs). The sorted and collected mEBs maintained pluripotency and selected mEBs successfully differentiated into three germ layers: endoderm, mesoderm, and ectoderm, thereby indicating the "biocompatibility" of the sorting device.

Non-homogenous swelling of polypyrole-based films in humid air was used to make actuator which reversibly bends folds and form the tubes.[47] The actuator generates a contractile stress up to 27 MPa, lift objects 380 times heavier than itself, and transports cargo 10 times heavier than itself.

In these examples, bending occurred when an electric field was applied and repeatable changes in shape require applying of alternating electric field. Alternatively, cyclical changes in shape of a homogeneous hydrogel[48] can be achieved by using the Belousov–Zhabotinsky (BZ) reaction.[49] The BZ reaction is well known as a non-equilibrium dissipative reaction and generates autonomous oscillations in the redox potential that changes the swelling properties of a hydrogel.[50] For example, Yoshida fabricated gels exhibiting autonomous peristaltic motion without external stimuli, prepared by copolymerizing temperature-responsive N-isopropylacrylamide with ruthenium tris(2,2′-bipyridine) (Ru(bpy)3) as a catalyst for the BZ reaction and were used for directed particle transport.[51] BZ reaction results in local swelling of the hydrogel that changes with time. As a result, a moving wave of swollen hydrogel is formed. The wave provides peristaltic motion of the adsorbed microparticles. In another approach, Maeda fabricated a self-oscillating gel actuator without external stimuli by producing a gradient structure, which generates a pendulum motion by fixing one edge of the gel (**Figure 8**).[52]

Summary: It was observed that homogeneous hydrogels typical undergo simple bending, which is caused by a 1D gradient of fields (concentration or temperature). The reason for such relatively simple behavior is that it is rather difficult to form complex spatial gradient of concentration, which can, for example, cause twisting. More complex behavior can, in principle, be achieved using oscillating reactions.

3.2.2. Inhomogeneous Hydrogels in a Homogeneous Field

This principle of hydrogel-based actuators is inspired by the actuating behavior of pine cones, wheat awn and the Venus flytrap, which are built by materials with different swelling properties.

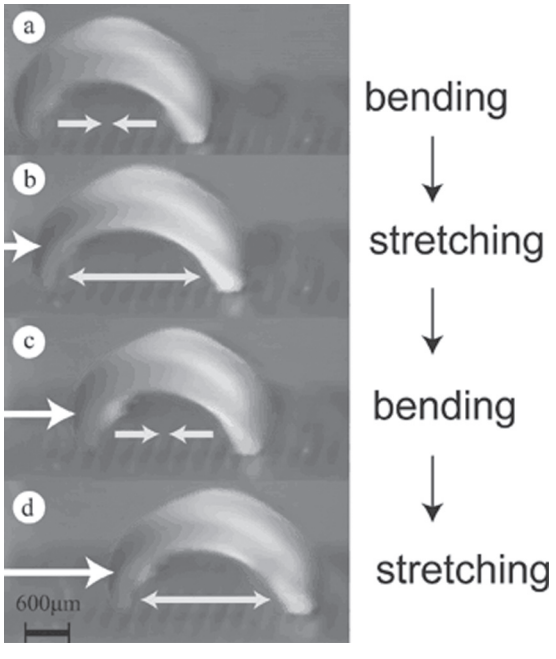

Figure 8. A gel actuator that can generate autonomous motility with a wormlike motion without external driving stimuli. The autonomous motion is produced by dissipating the chemical energy of an oscillating reaction occurring inside the gel. Even though the gel is completely composed of synthetic polymer, it shows an autonomous motion as if it were "alive". By coupling this with a ratchet mechanism, the gel walks by repeatedly bending and stretching itself like a looper. Reproduced with permission.[52b] Copyright 2007, Wiley-VCH.

Rods: The deformation of inhomogeneous materials has been known for a very long time and in 1925, Timoshenko[10] published a paper, which considered bending of a metal bilayer consisting of two metals with different thermal expansion coefficients. The deformation of non-hydrogel-based inhomogeneous inorganic materials is considered because the effects, which are produced by them, are similar to effects that can be achieved using hydrogels. Timoshenko assumed that the bilayer can bend in only one direction and results in a bilayer with uniform curvature:

$$\frac{1}{\rho} = \frac{6(\varepsilon_2 - \varepsilon_1)(1+m)^2}{h\left(3(1+m)^2 + (1+mn)\left(m^2 + \frac{1}{mn}\right)\right)} \quad (1)$$

$$\frac{E_1}{E_2} = n \quad (2)$$

$$\frac{a_1}{a_2} = m \quad (3)$$

where E_x are the elasticity modulus, a_x are the thickness of the layers, h is the total thickness ($h = a1+a2$), ε is the stress of the films, ρ is the radius of curvature. From Equations (1–3), the radius of curvature is inversely proportional to the film stress. Moreover, the radius of curvature first decreases and then increases with the increase in m. The resultant curvature is not very sensitive to the difference in stiffness between the two layers and is mainly controlled by the actuation strain and the layer thickness.

Similar to bimetal strips, hydrogel-based ones consisting of two kinds of hydrogel rods are able to bend in different direction depending on the swelling properties of polymers (**Figure 9**).[53]

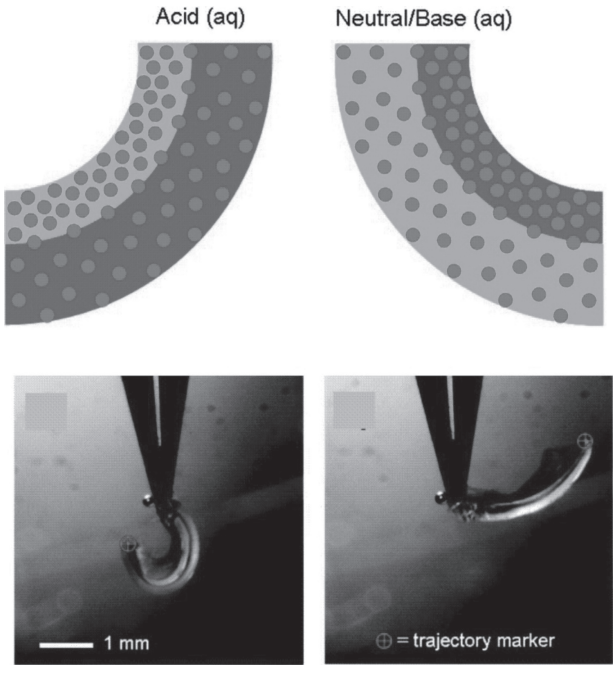

Figure 9. Bending of a biopolymer strip by positively and negatively charged polyelectrolytes. Reproduced with permission.[53a] Copyright 2007, American Chemical Society.

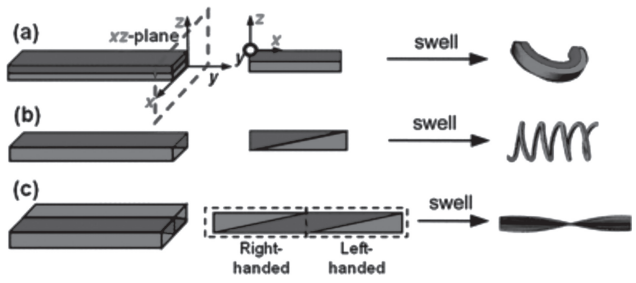

Figure 10. Schematic illustrations of a) bending, b) polypeptide -type twisting, c) DNA-type twisting actuators and d) formation of sharp hinges. Reproduced with permission.[55] Copyright 2011, Royal Society of Chemistry.

The first report of bending of a hydrogel bilayer rod, consisting of thermoresponsive part and non-thermoresponsive one, was published by Hu and co-workers in 1985.[54] They demonstrated that rods bend due to shrinking of thermoresponsive hydrogels when the temperature changes.

The bilayer rod with constant ratio between thicknesses of each layer along the sample bends in one direction (**Figure 10**a). By making a sloped bilayer structure, the planar structure described in Figure 10b can be bended along the y-axis as well as be twisted around this axis when one of the layers is asymmetrically expanded in a specifically selected solvent. When the bilayer actuating device with triangular layers with respect to the y-axis is swollen, a helical-type actuating sensor can be formed. A double twisted helical photonic actuator can be formed as shown in Figure 10c. The double twist actuating behavior is due to the competition of the twisting powers between the right-handed and the left-handed polypeptide-like helical structures.[55]

Turcaud and co-workers simulated deformation of rods with different geometry and asymmetry.[56] For constant cross-sections, it is possible to achieve planar bending (**Figure 11**a) or twisting when the material distribution breaks some of symmetry elements of the initial shape, preserving one mirror

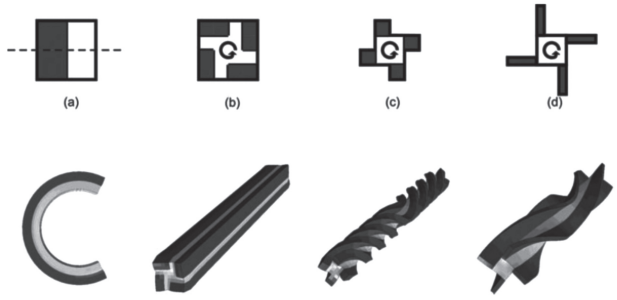

Figure 11. Simulated actuation for several cross-sections with passive/active areas ratio of 50:50: (from left to right). a) classical bilayer bending in its mirror plane; b) closed fourfold cross-section with bilayer repetitive unit cell remains straight; c) opened fourfold cross-section with bilayer repetitive unit cell shows huge twisting; d) opened fourfold cross-section with bigger moment of inertial shows less twisting than (c). Reproduced with permission.[56] Copyright 2011, Carl Hanser Verlag.

plane or one rotational axis. Twisting is more sensitive to other geometrical factors. In the case of compact cross-section (Figure 11b), no actual twisting is observed despite the fourfold rotational symmetry axis. However, the augmentation of free-border with the volume ratio of the two phases staying equal triggers twisting (Figure 11c). The moment of inertia of the cross-section relates inversely to the amount of twisting (Figure 11d). The eccentricity of the expanding region relative to the geometric centre of the cross-section is proportional to the degree of twisting.

Bending of Hydrogel Films With Vertical Swelling Gradients: Deformation of films is more complex than the deformation of rods. The Timoshenko equation applies to a beam bending in only one direction, does not predict the bending direction and is applicable for reversible elastic deformations. More recent models have considered complex bending of a bilayer in two dimensions. Mansfield found analytical solutions for large deflections of circular[57] and elliptical[58] plates having lenticular cross sections with a temperature gradient through the thickness. For small gradients, the plates formed spherical caps, curved equally in all directions. At a critical gradient, a configuration with greater curvature in one direction became more favorable. Because of the lens-shaped thickness profile, even though the elliptical plate had a major axis, it showed no preferred direction for bending even for large deflections. Freund determined the strain at which a spherical cap, formed by circular bilayer of uniform thickness, becomes unstable using low order polynomial solutions and finite element simulations.[59] Later Smela and co-workers showed that short-side bending of inorganic bilayer was preferred in the case of free homogeneous actuation and that this preference increased with aspect ratio (ratio of length to width of a rectangular pattern)[60] (**Figure 12**). Li and co-workers[61] and Schimdt[62] experimentally demonstrated the opposite scenario, namely a preference for long-side bending, in the case where bilayers are progressively etched from a substrate.

In inorganic bilayer systems, the active component undergoes relatively small volume changes or actuation strains, which are nearly homogeneous over the whole sample. Hydrogels, however, demonstrate considerably different properties. First, hydrogels undergo large volume changes (up to 10 times) upon swelling and contraction. Second, the swelling of a hydrogel is often kinetically limited: due to slow diffusion of water through a hydrogel, the parts which are closer to the edges swell first while the parts which are closer to the center of the films swell later.

It was found that when the radius of curvature is small, bending of the films leads to their folding and formation of 3D structures, such as tubes.[63] We investigated the bending/folding of rectangular stimuli-responsive hydrogel-based polymer bilayers with different aspect ratios and relative thicknesses placed on a substrate (**Figure 13**).[64] It was found that long-side folding dominates at high aspect ratios (ratio of length to width) when the width is comparable to the circumference of the formed tubes, which corresponds to a small actuation strain. Folding from all sides occurs for a higher actuation strain, namely when the width and length considerably exceed the deformed circumference. In the case of moderate actuation, when the width and length are comparable to the deformed

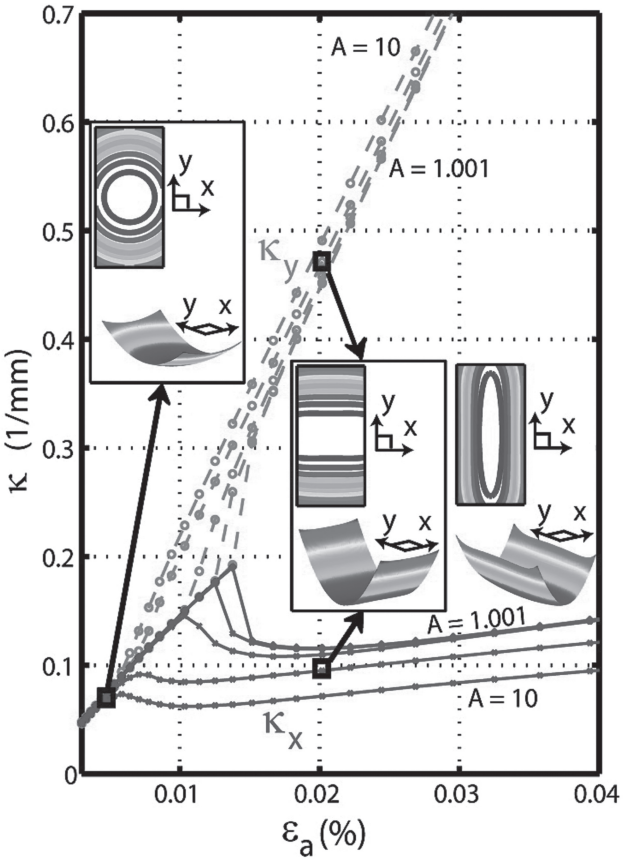

Figure 12. Simulations of curvature of free-standing inorganic bilayer as a function of actuation strain εa. The insets show shapes for A (ratio of length to width of the film) = 2 at the indicated εa; the out-of-plane z axis is greatly exaggerated for illustration. The colors go from blue to red as the z displacement increases. Simulation show that above threshold strain short side rolling dominates. Reproduced with permission.[60] Copyright 2011, American Chemical Society.

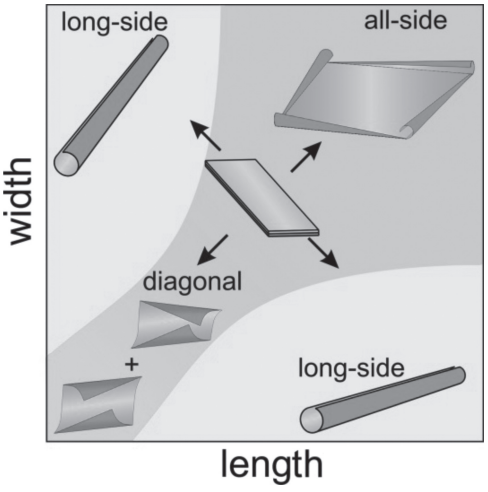

Figure 13. Different scenarios of deformation of polymer bilayers on a substrate depending of the width and length. Adapted with permission.[64b] Copyright 2012, American Chemical Society.

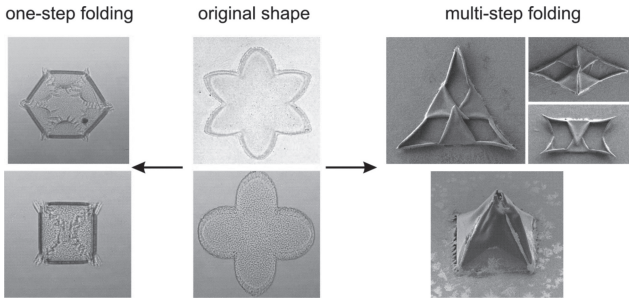

Figure 14. Results of one- and multi-step folding of four- and six-arm stars. Reproduced with permission.[66,70] Copyright 2011, Royal Society of Chemistry; Copyright 2013, Wiley-VCH.

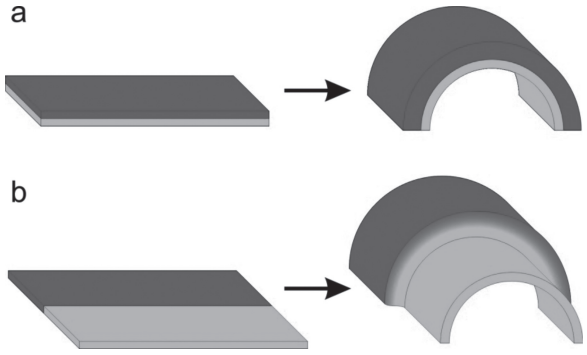

Figure 15. a) Bending of a "classical" bilayer and b) rectangular strips divided into one high- and one low-swelling regions. Dark blue is swelling hydrogel, light blue does not swell. Reproduced with permission.[72] Copyright 2013, Taylor & Francis.

circumference, diagonal rolling is observed. Short-side folding was observed very rarely and in combination with diagonal bending. In fact it was observed that bilayers placed on a substrate start to roll from corners due to quicker diffusion of water. Folding from the long-side starts later but dominates at high aspect ratios in agreement with energetic considerations. It was showed experimentally and by modeling that the main reasons causing a variety of rolling scenarios are (i) non-homogeneous swelling due to the presence of the substrate and (ii) adhesion of the polymer to the substrate. On the other hand, films, which are floating in solution, bend along their short side and formed scrolls.

One of the parameters, which determines the shape of a formed 3D object is the 2D shape of the polymer films. For example, tubes are formed from rectangle bilayers[63–65] (Figure 13). Envelope-like capsules with rounded corners or nearly spherical ones are formed the homogeneous star-like polymer bilayers with four and six arms, respectively (**Figure 14**, left).[65d,65e,66] Importantly, in many cases folding runs in one step. Step-by-step folding of different elements of self-folding films can be achieved by local activation of selected areas of self-folding films by light.[67] Another possibility is to use two or more kinds of active material which are sensitive to different signals. Gracias and co-workers demonstrated two-step deformation of patterned films where the active elements are two kinds of biodegradable polymers. Each of these polymers is degraded by specific enzyme. As a result, the film folds when the first enzyme is added and unfolds when the second one is added.[68] On the other hand, there are reports that folding in nature can have a very complex character, which strongly depends on the geometry and swelling path[69] and may result in multi-step folding (development of curvature in different directions).[2a] Recently, we demonstrated that the shape of isotropic polymer bilayers is able to direct folding in a sophisticated manner, leading to even more complex hierarchical folding than in nature. In particular, homogeneous bilayer films can undergo sequential steps of folding by forming various 3D shapes with sharp hinges (Figure 14, right). Experimental observations lead us to derive four empirical rules backed up by theoretical understanding as well as simulations. It was demonstrated how those rules can be used to direct the folding of edge-activated polymer bilayers through a concrete example: the design of a pyramid.[70]

Bending of Hydrogels Films with Lateral Swelling Gradients: Similar to bilayers, hydrogels with lateral gradients of swelling properties are also able to deform. They form complex figures with Gaussian curvature.[42] Similar to this work, Hayward and Santangelo investigated folding of patterned rectangular strips divided into one high- and one low-swelling region, which can be characterized as a thick but narrow bilayer.[71] When swollen in an aqueous medium, it does not bent to the side of the less swelling component that is the case of "classical" bilayer discussed by Timoshenko (**Figure 15**a), but rolls into a three-dimensional shape consisting of two nearly cylindrical regions connected by a transitional neck (Figure 15b).

Santangelo and Hayward further extended investigation of hydrogel films which consist of multiple areas with different swelling properties. The hydrogel was patterned using so-called halftone gel lithography using only two photomasks, wherein highly cross-linked dots embedded in a lightly cross-linked matrix provide access to nearly continuous and fully two-dimensional patterns of swelling. This method is used to fabricate surfaces with constant Gaussian curvature (spherical caps, saddles, and cones) or zero mean curvature (Enneper's surfaces), as well as more complex and nearly closed shapes (**Figure 16**)

Similar to the work of Hayward and Santangelo, Kumacheva and co-workers investigated deformation of hydrogel films formed by multiple regions with different swelling properties.[74] They demonstrated that the films are able to undergo multiple shape transitions when different polymers are swollen and shrunk. Thus, the polyelectrolyte film can be unfolded when there is no salt in solution, moderate increase of the ionic strength leads to folding and formation of tube, further increase of ionic strength results in unfolding of the film.

Snap-Buckling Deformation: In all these examples of hydrogels with vertical and later swelling gradients and in most plants movement occurs relatively slowly. Some plants such as the Venus flytrap, however, are able to move very quickly, which is due to a swelling-induced snap-buckling between two stable shapes. For snap-buckling instability, it is essential for the device to have directional swelling capability in addition to a doubly curved shape. The Venus flytrap, for instance, actively regulates the internal hydraulic pressure to bend its leaves in

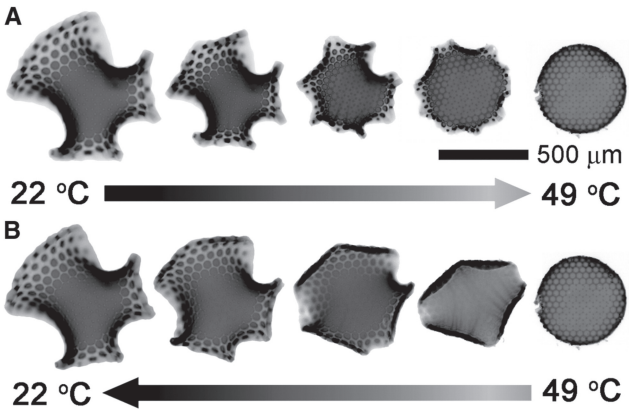

Figure 16. Thermal actuation of patterned sheets. a) When the temperature of the aqueous medium is increased, the hybrid Enneper's surface deswells and recovers its flat shape by 49 °C. b) Upon lowering the temperature to 22 °C the disk swells back to the initial hybrid shape through a different pathway. Initial thickness and disk diameter are 7 and 390 μm, respectively. Reproduced with permission.[73] Copyright 2012, AAAS.

a direction perpendicular to the midlib. From a mechanical point of view, the leaf is an elastic shell with a doubly curved shape. When bent along one axis only, an elastic body becomes stretched as a result of bending-stretching coupling of a doubly curved plate, thereby storing elastic energy. As the leaf further deforms and passes through the energy barrier, this stored elastic energy is instantaneously released and converted into kinetic energy, creating a rapid trap closure. Fang and co-workers [75] designed and fabricated a hydrogel device with a doubly curved shape to incorporate elastic instability. Unlike other hydrogel systems where the entire device needs to be immersed in solvent for actuation, swelling in this device takes place locally around the channels by direct solvent delivery. Therefore, a desired motion can be obtained by embedding channels where swelling is needed. The swelling of the device needs to be controlled in such a way that the curvature is actively manipulated only in one direction while the curvature in the other direction remains passive. To achieve directional swelling of a doubly curved hydrogel device, microfluidic channels were aligned vertically with spacing in between. Once supplied to the channels, the solvent diffuses out in all directions around it. Swelling in lateral direction is negligible within a short period of actuation time since the solvent diffusion speed is finite. On the contrary, swelling along the channels can quickly cause significant amount of bending in the vertical direction as the diffusion length in thickness direction is relatively short. Therefore, local swelling around the aligned channels makes the doubly curved device bend only along the vertical axis and, as a result, snap-buckling occurs. Similarly, the device snaps back to the original shape during de-swelling (**Figure 17**).

Summary: It was shown that inhomogeneous films with later and vertical gradients of swelling properties are able to fold and form various 2D and 3D objects. The shape of the formed objects is determined by the character of the gradient of swelling properties, size of the film, and its shape. The folding may occur in one step or in multiple steps. It was also demonstrated that folding can be relatively slow and, thus, mimics actuation mechanism in pine cones or can be very fast, mimicing actuation mechanism in the Venus flaytrap.

3.2.3. Application of Inhomogeneous Deformation of Hydrogels

Actuators: One possible kind of application of inhomogeneous hydrogels is bending actuators.[76] For example, AFM cantilevers coated on one side with hydrogel bend depending on the swelling state of the hydrogel and can be used for design of sensors.[77] In this way, pH-,[77a] temperature-, ion-[78] and biosensors[77b] were developed. Bashir and co-workers fabricated bending cantilever using PEG-based hydrogel with seeded cardiomyocytes, which were derived from neonatal rats.[79] These cantilevers were used as a mechanical sensor to measure the contractile forces of cardiomyocyte cell sheets and as an early prototype for the design of optimal cell-based biohybrid actuators.

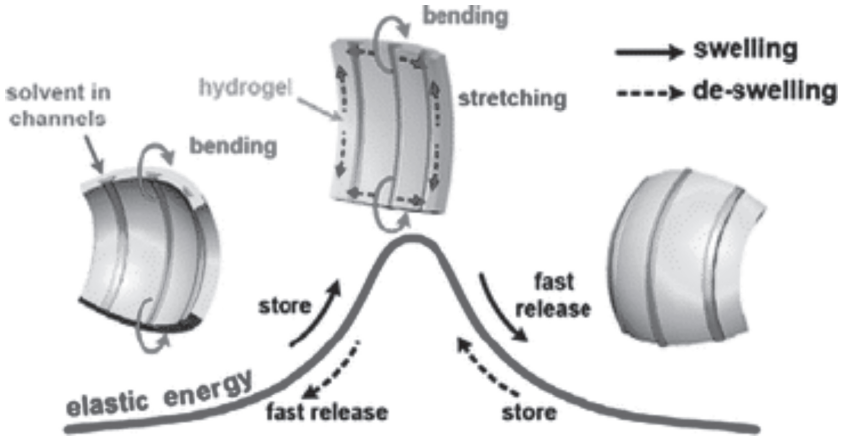

Figure 17. Swelling-induced snap-buckling in a doubly curved hydrogel device with embedded microfluidic channels. Scale bar indicates 100 mm. Reproduced with permission.[75] Copyright 2010, Royal Society of Chemistry.

Yu and co-workers used bending of bilayers for design of biomimetic check valve that allows for the directional control of fluid (**Figure 18**).[80] The valve consists of a bistrip formed by pH sensitive poly(HEMA-AA) hydrogel and a pH-indifferent poly(HEMA) hydrogel. Back pressure closes the leaflets, thereby restricting backflow, whereas forward pressure opens the leaflets and allows fluid to pass. The valve activates and deactivates in response to solution pH due to the use of a pH-responsive hydrogel in the leaflets. At high pH, the valve is functional and at low pH the leaflets contract to close the valve. Therefore, the valve not only functions as a one-way check valve, but also provides the ability to call the valve into service when desired. Similar check valves were found in mammalian veins.

In fact, bending can easily be transformed in walking or swimming by applying cyclical

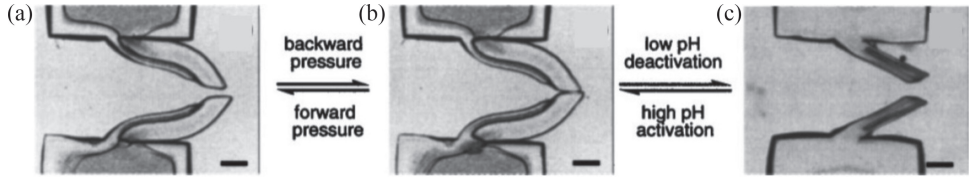

Figure 18. Smart biomimetic hydrogel valve based on hydrogel bistrip. When exposed to pH = 8 phosphate buffer, the bistrip hydrogel changes its size and shape to form a normally closed check valve (b); when exposed to pH = 3 buffer, the valve is deactivated due to shrinking (c). The activated valve allows forward fluid flow when forward pressure reaches a threshold value (a) while resisting backward flow (b). Scale bars are 500 μm. Reproduced with permission.[80] Copyright 2001, American Institute of Physics.

stimuli. In 1992 Osada and co-workers reported deformation of polyelectrolyte hydrogel immersed in surfactant solution causing swelling of the hydrogel.[81] The deformation of the hydrogel was due to complexing of the surfactant with the charged groups in the gel. Swelling occurred due to osmotic pressure changes and ions freely moving in the gel and solution. The hydrogel bends towards the cathode that allows to control direction of bending by polarity of applied voltage. Positive ions in the surfactant solution moved to the cathode and complex there. Switching of the polarity led to release of the surfactant. On the other hand, surfactant molecules complexed with charged group on the other side of the hydrogel that resulted in change of the bending direction. Thus, the gel demonstrated bending and stretching upon cyclic change in the polarity of the applied voltage. The specific deformation of hydrogel allowed its walking at a speed of 15 mm/min. Similar to this work, Sun and co-workers developed macroscopical hydrogel-based actuating system, which is able to walk on ratchet substrate. The system is based on bending of a hydrophobic (Norland Optical Adhesive 63)–hydrophilic (thermally crosslinked poly(acrylic acid)/PAA)/poly(allylamine hydrochloride)) bilayer in response to a change in humidity (**Figure 19**).[82] This bilayer actuator could drive a walking device carrying a load 120 times heavier than the actuator and to walk steadily on a ratchet substrate under periodic alternation of the relative humidity (RH) between 11 and 40%.

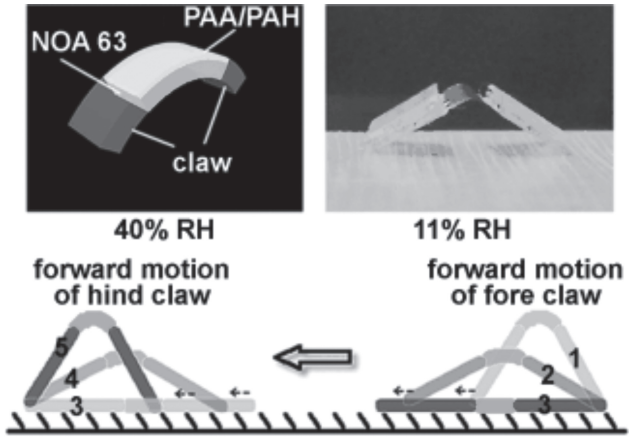

Figure 19. Walking device based on a polyelectrolyte multilayer film that can drive a walking device carrying a load 120 times heavier than the actuator and can walk steadily on a ratchet substrate under periodic alternation of the relative humidity (RH) between 11 and 40% (see picture). NOA 63: Norland Optical Adhesive 63, PAA: poly(acrylic acid), PAH: poly(allylamine hydrochloride). Reproduced with permission.[82] Copyright 2011, Wiley-VCH.

Hydrogel-based actuators are also able to swim when their shape changes cyclically. Lee and co-workers used inhomogeneous deformation of hydrogels and fabricated pH-sensitive hydrogel actuators mimicking the shape and the swimming motion of octopus and sperm (homogeneous hydrogel in electric field).[83] Such aquabots are able to produce directional motion in response to change of electrochemical potential and can be potentially used for biomedical applications to sense and destroy certain microorganism. Jager and co-workers demonstrated more complex actuation on the example of conjugated polymer actuators formed by bilayer consisting of polypyrrole and metal.[84] They showed that such bilayer actuators are able to operate in aqueous media, which is highly desirable for bioanalytical applications or to capture and release particles.[85] Whitesides, Parker and co-workers designed swimming biohybrid materials from engineered tissue and synthetic polymer thin film. The construct was built by culturing neonatal rat ventricular cardiomyocytes on PDMS film micropatterned with ECM (what's ECM) to promote spatially ordered, two-dimensional myogenesis. The centimeter-scale constructs performed diverse gripping, pumping, walking and swimming with good spatial and temporal control and were able to generate forces as high as 4 millinewtons per square millimeter.[86] Later on, Parker and Dabiri reported construction of a freely swimming jellyfish from chemically dissociated rat tissue and silicone polymer as a proof of concept (**Figure 20**).[87] The constructs, termed 'medusoids', were designed with computer simulations and experiments to match key determinants of jellyfish propulsion and feeding performance by quantitatively mimicking structural design, stroke kinematics and animal-fluid interactions. The combination of the engineering design algorithm with quantitative benchmarks of physiological performance suggests that this strategy is broadly applicable to reverse engineering of muscular organs or simple life forms that pump to survive. Similar approach was recently used by Bashir and coworkers to fabricate walking biological machines consisting of polymer layer with attached cardiac cell sheet.[88]

Self-Folding Films: In examples given above, the deformation of a hydrogels was used to generate mechanical force that allows development of moving systems. Deformation of hydrogel can also lead to considerable change of their shape this is used for design complex 2D and 3D systems in an origami-inspired self-folding concept. Utilization of hydromorphic folding of hydrogels for design of structured materials is highly attractive: it allows very simple, template-free fabrication of very

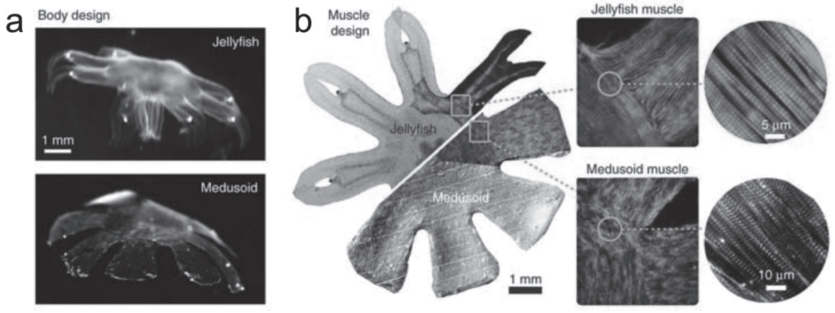

Figure 20. a) Body design of jellyfish (top) and free-swimming medusoid construct (bottom). Comparison demonstrates similar geometry and dimensions but also illustrates that the medusoid constitutes a simplified version of a jellyfish, reduced to elements necessary for propulsive function. b) Jellyfish 2D muscle architecture (top) was reverse-engineered in medusoids (bottom). Left: Composite brightfield image overlaid with F-actin stain (green) of muscle cell monolayer. Square inset: Close-up on muscle organization at lobe-body junction; F-actin stain (green). Reproduced with permission.[87] Copyright 2011, Nature Publishing Group.

complex repetitive 2D and 3D patterns,[89] which can hardly be prepared using other very sophisticated methods, such as two-photon and interference photolithography (**Figure 21**). One of the advantages of self-folding hydrogels is the possibility of quick, reversible and reproducible fabrication of 3D hollow objects with controlled chemical properties and morphology of both the exterior and interior. Most of the efforts until now were focused on inorganic self-folding materials.[16a,62,90] On the other hand, there are many factors, which make polymer-based self-folding films particularly attractive:[16b,91] i) there is a variety of polymers sensitive to different stimuli that allow design of self-folding films, which are able to fold in response to various external signals; ii) there are many polymers changing their properties in physiological ranges of pH and temperature, as well as polymers sensitive to biochemical signals; iii) there is a variety of biocompatible and biodegradable polymers. These properties make polymer-based self-folding films very attractive for biotechnological applications; iv) polymers undergo considerable and reversible changes of volume that allow design of systems with reversible folding; v) fabrication of 3D structures with sizes ranging from hundreds of nanometers to centimeters is possible.

There are numerous reports describing fabrication of self-folding films with different responsive properties. For example, there are pH-responsive systems based on polyelectr olytes,[63,65c,65e,92,94] thermoresponsive based on gradient of thermal expansion,[65a,65b] melting of polymer,[95,96] thermoresponsive polymers[64a,66]; polymers responsive to sol vents,[40,55,65e,92] electric signal,[85a,86,97] enzymes,[68] and light (based on light-to-heat conversion)[98]

One field of application of self-folding polymer thin films is controlled encapsulation and release of drugs, particles, and cells. Kalaitzidou demonstrated reversible adsorption-desorption of fluorescently labeled polyethyleneglycol, which was considered as model drug, inside PDMS-gold tubes at 60–70 °C.[65a] Similar, Gracias and co-workers showed irreversible encapsulation of yeast cells inside self-folding SU8-PCL films upon heating above 60 °C.[95] Poly-(N-isopropylacrylamide)-based self-folding films were also suitable for reversible encapsulation of particles and yeast cells.[64a,66] Cells were encapsulated upon cooling below 30 °C and could be released from the film, which is unfolded above 30 °C (**Figure 22**a). This encapsulation

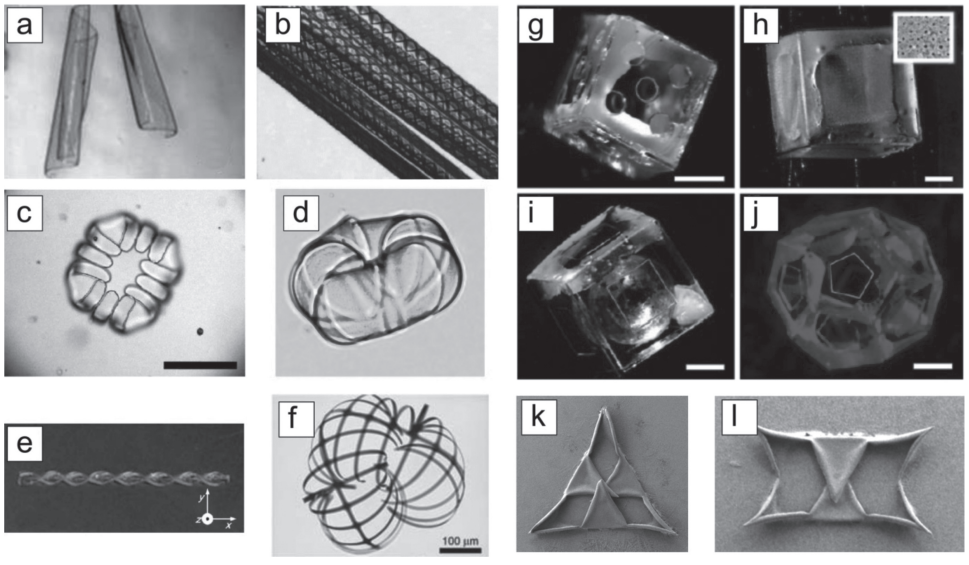

Figure 21. Examples of self-folding polymer films with different shapes: a,b) tubes. Reproduced with permission[63,65b] Copyright 2005, Wiley-VCH Verlag; c,d) capsules. Reproduced with permission.[65d,66] Copyright 2007, Wiley-VCH, Copyright 2013, Taylor & Francis; e) helix. Reprocued with permission.[55] Copyright 2011, Royal Society of Chemistry; f) hierarchically-shaped tube. Reproduced with permission.[92] Copyright 2011, Wiley-VCH; g–i) cubes with porous walls. Reproduced with permission.[93] Copyright 2011, Springer; j) dodecahedron. Reproduced with permission.[93] Copyright 2011, Springer; k,l) complex structures obtained by folding of six-armed stars. Reproduced with permission.[70] Copyright 2013, Wiley-VCH.

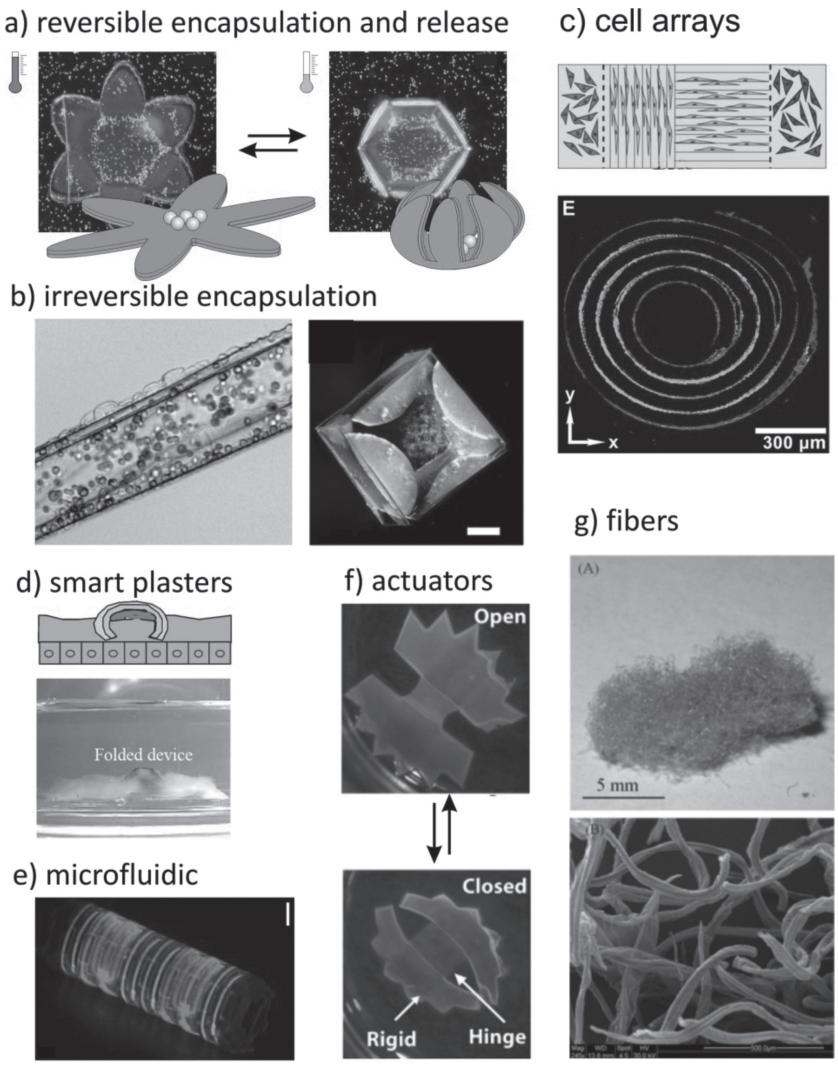

Figure 22. Examples of applications of self-folding polymer films: a) reversible encapsulation and release of yeast cells inside thermoresponsive self-folding capsules. Reproduced with permission.[66] Copyright 2010, Royal Society of Chemistry; b) irreversible encapsulation of cells–yeast cells encapsulation inside fully biodegradable self-rolled film (left: Reproduced with permission.[99] Copyright 2011, American Chemical Society) and stained fibroblast cells encapsulated within a non-porous polymeric container (right: Reproduced with permission.[110] Copyright 2010, Springer; c) array of multiple cells inside self-rolled prestressed PDMS film (Reproduced with permission.[106] Copyright 2012, Wiley-VCH; d) smart plasters which direct diffusion of drugs and prevent their leakage (Reproduced with permission.[65c] Copyright 2006, Elsevier; e) 3D mirofludic device obtained by folding (Reproduced with permission.[108] Copyright 2011, Nature Publishing Group; f) actuator with hinges folding in changing pH and ionic strength (Reproduced with permission.[94c] Copyright 2010, Elsevier; g) optical (top) and electron microscopy (bottom) images of fibrous material obtained from self-folding polymer films (Reproduced with permission.[109] Copyright 2012, Wiley-VCH.

and release is completely reversible and could be repeated many times. Very recently, fully biodegradable self-folding films, which consist of commercially available biodegradable polymers, were also used to encapsulate cells (Figure 22b).[99] It was also found out that cells are able to stimulate folding of patterned film.[100] In fact, there are many approaches which can be used for encapsulation of cells including LbL, microfluidic technique and controlled precipitation. The advantage of the self-folding approach is the possibility of reversible encapsulation and release. Self-folded objects with nanoporous walls and encapsulated cells were suggested as prototype for artificial pancreas. Small molecules, such as glucose and dissolved oxygen, are able to pass through the pores, while larger ones, such as antibodies, are unable to do so. This size-selective permeability of self-folded capsules makes it possible to avoid the immune response what is highly demanded during transplantation of pancreas cells.[101] Gracias and co-workers used rigid metal-made self-folding microgrippers for capturing pieces of tissues and their controlled transport. Such systems are particularly attractive for non-invasive biopsy.[96c,102] Self-folded objects were used as scaffolds for the fabrication of 3D cellular constructs.[103] Controlled release of small molecules through the pores of self-folded microconstructs was used to spontaneously organize cells in a 3D environment[104] that potentially allows fabrication of 3D scaffolds for tissue engineering.[105] For example, self-rolling prestressed PDMS films with adsorbed cells of different kinds were used to make tubular structures mimicking the structure of blood vessels (Figure 22c).[106]

Self-folding films can also be used as smart plasters (Figure 22d). Lee demonstrated this concept with the example of a millimerter size poly(methyl methacrylate)–poly(2-hydroxyethyl methacrylate) bilayer with attached mucoadhesive drug layer. The non-swelling PHEMA layer serves as a diffusion barrier minimizing any drug leakage in the intestine. The resulting unidirectional release provides improved drug transport through the mucosal epithelium. The functionality of this device was successfully proven in vitro using a porcine small intestine.[65c]

There are several non-biorelated examples of applications of self-folding polymer films. Deposition of patterned metal on the polymer bilayer allowed fabrication of self-rolled tubes with patterned conductive inner wall.[63] In another examples, pyrolysis of polystyrene-poly(4-vinyl pyridine)-polydimethylsiloxane trilayer[94a] and polystyrene–poly(4-vinyl pyridine)/resorcinol bilayer[107] was used for the fabrication of silica and carbon tubes, respectively. Gracias used self-folding polymers films to fabricate self-assembled curved microfluidic networks (Figure 22e)[108] and designed smart actuating systems mimicking opening and closing of the Venus flytrap by using pH responsive polymer, which form a hinge between two polymer films (Figure 22f).[94c] Very recently, Luchnikov and co-workers fabricated fibers with hollow interiors using scratched self-folding polymer films (Figure 22g).[109]

4. Conclusions and Outlook

Nature offers myriads of ideas for the design of advanced materials with novel properties. The principles of movement in plants have been successfully transferred in the design of actively-moving hydrogel-based materials. In different applications, swelling/shrinking of stimuli-responsive hydrogels is used to generate forces, and to change their volume and shape. Experiments show that hydrogel actuators can produce simple motion, such as homogeneous increase of volume, more complex bending and twisting as well as highly complex origami-like folding.

One can distinguish: (i) homogenous hydrogels with homogenous in all directions deformation; (ii) homogenous hydrogels with inhomogeneous in deformation and (iii) inhomogeneous hydrogels with inhomogeneous in deformation. Behavior of the first type is similar to swelling of cells. Behavior of the second type has no examples in nature. Behavior of third type mimics movements of pine cones, wheat awn, Venus flytrap etc. The third type of hydrogel actuator demonstrates the most complex scenarios of deformation such as bending, twisting, one- and multi-step folding leading to formation of complex 2D and 3D structures. In particular, one of the recent trends is to develop approaches for multi-step hierarchical actuation. One way to achieve multi-step actuation is to use several hydrogels sensitive to several stimuli or site-selective activation of different elements of self-folding films. In these cases either manufacturing or folding becomes more time-consuming. Another approach, which is inspired by nature, is to use inhomogeneity of the swelling path that allows very complex folding in a way that star-arm bilayers build pyramids with sharp hinges. One can even imagine the use of complex deformation of hydrogels for folding of printed origami structures[111] in order to achieve higher degree of complexity.

The complex movement/deformation of hydrogels has been successfully applied for the design of active elements for microfluidic devices, materials and devices with tunable optical properties, switchable surface, engineering of biomaterials, cell encapsulation, 3D microfluidic systems. There are also very interesting examples of "cyborg" devices build from living cells and synthetic materials. These first experiments give hope for the development of biomimetic polymer materials, which can be completely integrated into living organisms and be controlled by them. It was also demonstrated that self-folding hydrogel-based films are very promising for the design of biomaterials, controlled encapsulation and release of drugs and cells. In particular, due to their softness, better biocompatibility, possible biodegradability and easy manufacturing, hydrogel actuators can be applied in the fields of microelectronics and bio-microelectronics for in vivo applications.

Acknowledgements

The author is grateful to DFG (Grant IO 68/1-1) for financial support. Georgi Stoychev is acknowledged for helpful comments on the manuscript.

Received: December 13, 2012
Revised: March 27, 2013
Published online: June 5, 2013

[1] a) F. Tama, C. L. Brooks, *Annu. Rev. Biophys. Biomol. Struct.* **35**, **2006**, 115–133; b) A.-L. Barabasi, Z. N. Oltvai, *Nat. Rev. Genet.* **2004**, *5*, 101–113; c) J. Bath, A. J. Turberfield, *Nat. Nanotechnol.* **2007**, *2*, 275–284; d) P. Schwille, S. Diez, *Crit. Rev. Biochem. Mol. Biol.* **2009**, *44*, 223–242; e) W. J. Crookes, L. L. Ding, Q. L. Huang, J. R. Kimbell, J. Horwitz, M. J. McFall-Ngai, *Science* **2004**, *303*, 235–238; f) R. Vaia, J. Baur, *Science* **2008**, *319*, 420–421.

[2] a) M. J. Harrington, K. Razghandi, F. Ditsch, L. Guiducci, M. Rueggeberg, J. W. C. Dunlop, P. Fratzl, C. Neinhuis, I. Burgert, *Nat. Commun.* **2011**, *2*, 337; b) P. Fratzl, F. G. Barth, *Nature* **2009**, *462*, 442–448.

[3] a) I. Burgert, P. Fratzl, *Philos. Trans. R. Soc. A* **2009**, *367*, 1541–1557; b) R. Elbaum, L. Zaltzman, I. Burgert, P. Fratzl, *Science* **2007**, *316*, 884–886; c) E. Reyssat, L. Mahadevan, *J. R. Soc., Interface* **2009**, *6*, 951–957.

[4] a) L. Ionov, *J. Mater. Chem.* **2010**, *20*, 3382–3390; b) I. Tokarev, S. Minko, *Soft Matter* **2009**, *5*, 511–524; c) Y. Qiu, K. Park, *Adv. Drug Delivery Rev.* **2001**, *53*, 321–339; d) W. T. S. Huck, *Mater Today* **2008**, *11*, 24–32; e) Z. Liu, P. Calvert, *Adv. Mater.* **2000**, *12*, 288–291; f) B. Kaehr, J. B. Shear, *Proc. Natl. Acad. Sci. USA* **2008**, *105*, 8850–8854.

[5] a) C. D. Jones, L. A. Lyon, *J. Am. Chem. Soc.* **2003**, *125*, 460–465; b) Z. Y. Meng, M. H. Smith, L. A. Lyon, *Colloid Polym. Sci.* **2009**, *287*, 277–285; c) S. Bhattacharya, F. Eckert, V. Boyko, A. Pich, *Small* **2007**, *3*, 650–657.

[6] a) S. K. Ahn, R. M. Kasi, S. C. Kim, N. Sharma, Y. X. Zhou, *Soft Matter* **2008**, *4*, 1151–1157; b) D. Buenger, F. Topuz, J. Groll, *Prog. Polym. Sci.* **2012**, *37*, 1678–1719.

[7] K. Haraguchi, K. Murata, T. Takehisa, *Macromolecules* **2011**, *45*, 385–391.

[8] J. M. Skotheim, L. Mahadevan, *Science* **2005**, *308*, 1308–1310.

[9] C. Dawson, J. F. V. Vincent, A.-M. Rocca, *Nature* **1997**, *390*, 668–668.

[10] S. Timoshenko, *J. Opt. Soc. Am. Rev. Sci. Instrum.* **1925**, *11*, 233–255.

[11] Y. Forterre, J. M. Skotheim, J. Dumais, L. Mahadevan, *Nature* **2005**, *433*, 421–425.

[12] D. Evangelista, S. Hotton, J. Dumais, *J. Exp. Biol.* **2011**, *214*, 521–529.

[13] J. W. C. Dunlop, R. Weinkamer, P. Fratzl, *Mater Today* **2011**, *14*, 70–78.

[14] D. P. Holmes, A. J. Crosby, *Adv. Mater.* **2007**, *19*, 3589–3593.

[15] A. G. Volkov, V. A. Murphy, J. I. Clemmons, M. J. Curley, V. S. Markin, *J. Plant Physiol.* **2012**, *169*, 55–64.

[16] a) T. G. Leong, A. M. Zarafshar, D. H. Gracias, *Small* **2010**, *6*, 792–806; b) L. Ionov, *Soft Matter* **2011**, *7*, 6786–6791.

[17] a) Y. Gong, M. Gao, D. Wang, H. Möhwald, *Chem. Mat.* **2005**, *17*, 2648–2653; b) C. Chang, B. Duan, J. Cai, L. Zhang, *Eur. Polym. J.* **2010**, *46*, 92–100; c) D. J. Gan, L. A. Lyon, *J. Am. Chem. Soc.* **2001**, *123*, 7511–7517.

[18] J. K. Oh, R. Drumright, D. J. Siegwart, K. Matyjaszewski, *Prog. Polym. Sci.* **2008**, *33*, 448–477.

[19] J. Rubio-Retama, N. E. Zafeiropoulos, C. Serafinelli, R. Rojas-Reyna, B. Voit, E. L. Cabarcos, M. Stamm, *Langmuir* **2007**, *23*, 10280–10285.

[20] a) J. S. Kim, N. Singh, L. A. Lyon, *Angew. Chem. Int. Ed.* **2006**, *45*, 1446–1449; b) J. Kim, M. J. Serpe, L. A. Lyon, *J. Am. Chem. Soc.* **2004**, *126*, 9512–9513.

[21] a) I. Gorelikov, L. M. Field, E. Kumacheva, *J. Am. Chem. Soc.* **2004**, *126*, 15938–15939; b) M. Agrawal, J. Rubio-Retama, N. E. Zafeiropoulos, N. Gaponik, S. Gupta, V. Cimrova, V. Lesnyak, E. Lopez-Cabarcos, S. Tzavalas, R. Rojas-Reyna, A. Eychmuller, M. Stamm, *Langmuir* **2008**, *24*, 9820–9824.

[22] a) K.-U. Jeong, J.-H. Jang, C. Y. Koh, M. J. Graham, K.-Y. Jin, S.-J. Park, C. Nah, M.-H. Lee, S. Z. D. Cheng, E. L. Thomas, *J.*

Mater. Chem. **2009**, *19*, 1956–1959; b) K. Ueno, K. Matsubara, M. Watanabe, Y. Takeoka, *Adv. Mater.* **2007**, *19*, 2807–2812; c) H. Fudouzi, Y. Xia, *Adv. Mater.* **2003**, *15*, 892–896; d) K. Matsubara, M. Watanabe, Y. Takeoka, *Angew. Chem. Int. Ed.* **2007**, *46*, 1688–1692.

[23] J. R. Lawrence, G. H. Shim, P. Jiang, M. G. Han, Y. Ying, S. H. Foulger, *Adv. Mater.* **2005**, *17*, 2344–2349.

[24] J. P. Ge, Y. X. Hu, Y. D. Yin, *Angew. Chem. Int. Ed.* **2007**, *46*, 7428–7431.

[25] K. Ueno, J. Sakamoto, Y. Takeoka, M. Watanabe, *J. Mater. Chem.* **2009**, *19*, 4778–4783.

[26] a) K.-F. Arndt, D. Kuckling, A. Richter, *Polym. Adv. Technol.* **2000**, *11*, 496–505; b) L. Dong, H. Jiang, *Soft Matter* **2007**, *3*, 1223–1230; c) D. J. Beebe, J. S. Moore, Q. Yu, R. H. Liu, M. L. Kraft, B.-H. Jo, C. Devadoss, *Proc. Natl. Acad. Sci. USA* **2000**, *97*, 13488–13493; d) D. T. Eddington, D. J. Beebe, *Adv. Drug Delivery Rev.* **2004**, *56*, 199–210.

[27] a) D. T. Eddington, R. H. Liu, J. S. Moore, D. J. Beebe, *Lab Chip* **2001**, *1*, 96–99; b) D. J. Beebe, J. S. Moore, J. M. Bauer, Q. Yu, R. H. Liu, C. Devadoss, B. H. Jo, *Nature* **2000**, *404*, 588–590; c) Z. Xuefeng, J. Hongrui, *Appl. Phys. Lett.* **2008**, *93*, 151101.

[28] a) A. Richter, D. Kuckling, S. Howitz, T. Gehring, K. F. Arndt, *J. Microelectromech. Syst.* **2003**, *12*, 748–753; b) A. Richter, S. Klatt, G. Paschew, C. Klenke, *Lab Chip* **2009**, *9*, 613–618.

[29] A. Richter, G. Paschew, *Adv. Mater.* **2009**, *21*, 979–983.

[30] A. Richter, G. Paschew, S. Klatt, J. Lienig, K. F. Arndt, H. J. P. Adler, *Sensors* **2008**, *8*, 561–581.

[31] L. J. Millet, E. A. Corbin, R. Free, K. Park, H. Kong, W. P. King, R. Bashir, *Small* **2012**, *8*, 2450–2450.

[32] a) I. Tokarev, I. Tokareva, S. Minko, *Adv. Mater.* **2008**, *20*, 2730–2734; b) V. Kozlovskaya, E. Kharlampieva, B. P. Khanal, P. Manna, E. R. Zubarev, V. V. Tsukruk, *Chem. Mat.* **2008**, *20*, 7474–7485; c) J. Li, X. Hong, Y. Liu, D. Li, Y. W. Wang, J. H. Li, Y. B. Bai, T. J. Li, *Adv. Mater.* **2005**, *17*, 163–166; d) M. Kuang, D. Wang, H. Möhwald, *Adv. Funct. Mater.* **2005**, *15*, 1611–1616.

[33] L. Dong, A. K. Agarwal, D. J. Beebe, H. Jiang, *Nature* **2006**, *442*, 551.

[34] A. Pelah, R. Seemann, T. M. Jovin, *J. Am. Chem. Soc.* **2006**, *129*, 468–469.

[35] H. Tekin, J. G. Sanchez, C. Landeros, K. Dubbin, R. Langer, A. Khademhosseini, *Adv. Mater.* **2012**, *24*, 5543–5547.

[36] a) B. Pokroy, A. K. Epstein, M. C. M. Persson-Gulda, J. Aizenberg, *Adv. Mater.* **2009**, *21*, 463–469; b) A. Sidorenko, T. Krupenkin, A. Taylor, P. Fratzl, J. Aizenberg, *Science* **2007**, *315*, 487–490; c) L. D. Zarzar, P. Kim, J. Aizenberg, *Adv. Mater.* **2011**, *23*, 1442–1446.

[37] A. Sidorenko, T. Krupenkin, J. Aizenberg, *J. Mater. Chem.* **2008**, *18*, 3841–3846.

[38] X. He, M. Aizenberg, O. Kuksenok, L. D. Zarzar, A. Shastri, A. C. Balazs, J. Aizenberg, *Nature* **2012**, *487*, 214–218.

[39] G. H. Kwon, Y. Y. Choi, J. Y. Park, D. H. Woo, K. B. Lee, J. H. Kim, S.-H. Lee, *Lab Chip* **2010**, *10*, 1604–1610.

[40] D. P. Holmes, M. Roche, T. Sinha, H. A. Stone, *Soft Matter* **2011**, *7*, 5188–5193.

[41] C. Ohm, M. Brehmer, R. Zentel, *Adv. Mater.* **2010**, *22*, 3366–3387.

[42] Y. Klein, E. Efrati, E. Sharon, *Science* **2007**, *315*, 1116–1120.

[43] a) F. Zhou, P. M. Biesheuvel, E. Y. Chol, W. Shu, R. Poetes, U. Steiner, W. T. S. Huck, *Nano Lett.* **2008**, *8*, 725–730; b) M. C. LeMieux, M. E. McConney, Y.-H. Lin, S. Singamaneni, H. Jiang, T. J. Bunning, V. V. Tsukruk, *Nano Lett.* **2006**, *6*, 730–734.

[44] T. Tanaka, I. Nishio, S. T. Sun, S. Uenonishio, *Science* **1982**, *218*, 467–469.

[45] M. Doi, M. Matsumoto, Y. Hirose, *Macromolecules* **1992**, *25*, 5504–5511.

[46] H. L. Lim, J. C. Chuang, T. Tran, A. Aung, G. Arya, S. Varghese, *Adv. Funct. Mater.* **2011**, *21*, 55–63.

[47] M. Ma, L. Guo, D. G. Anderson, R. Langer, *Science* **2013**, *339*, 186–189.

[48] D. Suzuki, T. Kobayashi, R. Yoshida, T. Hirai, *Soft Matter* **2012**.

[49] A. N. Zaikin, A. M. Zhabotinsky, *Nature* **1970**, *225*, 535–537.

[50] S. Maeda, Y. Hara, R. Yoshida, S. Hashimoto, *Int. J. Mol. Sci.* **2010**, *11*, 52–66.

[51] Y. Murase, S. Maeda, S. Hashimoto, R. Yoshida, *Langmuir* **2008**, *25*, 483.

[52] a) S. Maeda, Y. Hara, R. Yoshida, S. Hashimoto, *Macromol. Rapid. Commun.* **2008**, *29*, 401–405; b) S. Maeda, Y. Hara, T. Sakai, R. Yoshida, S. Hashimoto, *Adv. Mater.* **2007**, *19*, 3480–3484.

[53] a) P. D. Topham, J. R. Howse, C. J. Crook, S. P. Armes, R. A. L. Jones, A. J. Ryan, *Macromolecules* **2007**, *40*, 4393; b) S. Saha, D. Copic, S. Bhaskar, N. Clay, A. Donini, A. J. Hart, J. Lahann, *Angew. Chem. Int. Ed.* **2012**, *51*, 660–665; c) K. J. Lee, J. Yoon, S. Rahmani, S. Hwang, S. Bhaskar, S. Mitragotri, J. Lahann, *Proc. Natl. Acad. Sci. USA* **2012**, *109*, 16057–16062; d) K. K. Westbrook, H. J. Qi, *J. Intell. Mater. Syst. Struct.* **2008**, *19*, 597–607.

[54] Z. B. Hu, X. M. Zhang, Y. Li, *Science* **1995**, *269*, 525–527.

[55] K.-U. Jeong, J.-H. Jang, D.-Y. Kim, C. Nah, J. H. Lee, M.-H. Lee, H.-J. Sun, C.-L. Wang, S. Z. D. Cheng, E. L. Thomas, *J. Mater. Chem.* **2011**, *21*, 6824–6830.

[56] S. Turcaud, L. Guiducci, P. Fratzl, Y. J. M. Brechet, J. W. C. Dunlop, *Int. J. Mater. Res.* **2011**, *102*, 607–612.

[57] E. H. Mansfield, *Proc. R. Soc. A* **1962**, *268*, 316–237.

[58] E. H. Mansfield, *Proc. R. Soc. A* **1965**, *288*, 396–417.

[59] L. B. Freund, *J. Mech. Phys. Solids* **2000**, *48*, 1159–1174.

[60] S. Alben, B. Balakrisnan, E. Smela, *Nano Lett.* **2011**, *11*, 2280–2285.

[61] I. S. Chun, A. Challa, B. Derickson, K. J. Hsia, X. Li, *Nano Lett.* **2010**, *10*, 3927–3932.

[62] P. Cendula, S. Kiravittaya, I. Monch, J. Schumann, O. G. Schmidt, *Nano Lett.* **2011**, *11*, 236–240.

[63] V. Luchnikov, O. Sydorenko, M. Stamm, *Adv. Mater.* **2005**, *17*, 1177–1182.

[64] a) S. Zakharchenko, N. Puretskiy, G. Stoychev, M. Stamm, L. Ionov, *Soft Matter* **2010**, *6*, 2633–2636; b) G. Stoychev, S. Zakharchenko, S. Turcaud, J. W. C. Dunlop, L. Ionov, *ACS Nano* **2012**, *6*, 3925–3934.

[65] a) K. Kalaitzidou, A. J. Crosby, *Appl. Phys. Lett.* **2008**, *93*, 041910; b) B. Simpson, G. Nunnery, R. Tannenbaum, K. Kalaitzidou, *J. Mater. Chem.* **2010**, *20*, 3496–3501; c) H. Y. He, J. J. Guan, J. L. Lee, *J. Controlled Release* **2006**, *110*, 339–346; d) J. J. Guan, H. Y. He, L. J. Lee, D. J. Hansford, *Small* **2007**, *3*, 412–418; e) J. J. Guan, H. Y. He, D. J. Hansford, L. J. Lee, *J. Phys. Chem. B* **2005**, *109*, 23134–23137.

[66] G. Stoychev, N. Puretskiy, L. Ionov, *Soft Matter* **2011**, *7*, 3277–3279.

[67] K. E. Laflin, C. J. Morris, T. Muqeem, D. H. Gracias, *Appl. Phys. Lett.* **2012**, *101*, 131901.

[68] N. Bassik, A. Brafman, A. M. Zarafshar, M. Jamal, D. Luvsanjav, F. M. Selaru, D. H. Gracias, *J. Am. Chem. Soc.* **2010**, *132*, 16314–16317.

[69] a) H. Y. Liang, L. Mahadevan, *Proc. Natl. Acad. Sci. USA* **2011**, *108*, 5516–5521; b) H. Liang, L. Mahadevan, *Proc. Natl. Acad. Sci. USA* **2009**, *106*, 22049–22054.

[70] G. Stoychev, S. Turcaud, J. W. C. Dunlop, L. Ionov, *Adv. Funct. Mater.* DOI: 10.1002/adfm.201203245.

[71] J. Kim, J. A. Hanna, R. C. Hayward, C. D. Santangelo, *Soft Matter* **2012**, *8*, 2375–2381.

[72] L. Ionov, *Polym. Rev.* **2013**, *53*, 92–107.

[73] J. Kim, J. A. Hanna, M. Byun, C. D. Santangelo, R. C. Hayward, *Science* **2012**, *335*, 1201–1205.

[74] a) H. Thérien-Aubin, Z. L. Wu, Z. Nie, E. Kumacheva, *J. Am. Chem. Soc.* **2013**; b) Z. L. Wu, M. Moshe, J. Greener, H. Therien-Aubin, Z. Nie, E. Sharon, E. Kumacheva, *Nat. Commun.* **2013**, *4*, 1586.
[75] H. Lee, C. Xia, N. X. Fang, *Soft Matter* **2010**, *6*, 4342–4345.
[76] J. S. Randhawa, K. E. Laflin, N. Seelam, D. H. Gracias, *Adv. Funct. Mater.* **2011**, *21*, 2395–2410.
[77] a) R. Bashir, J. Z. Hilt, O. Elibol, A. Gupta, N. A. Peppas, *Appl. Phys. Lett.* **2002**, *81*, 3091–3093; b) J. Z. Hilt, A. K. Gupta, R. Bashir, N. A. Peppas, *Biomed. Microdevices* **2003**, *5*, 177–184.
[78] a) K. Liu, H. F. Ji, *Anal Sci* **2004**, *20*, 9–11; b) Y. Zhang, H.-F. Ji, G. M. Brown, T. Thundat, *Anal. Chem.* **2003**, *75*, 4773–4777.
[79] V. Chan, J. H. Jeong, P. Bajaj, M. Collens, T. Saif, H. Kong, R. Bashir, *Lab Chip* **2012**, *12*, 88–98.
[80] Q. Yu, J. M. Bauer, J. S. Moore, D. J. Beebe, *Appl. Phys. Lett.* **2001**, *78*, 2589–2591.
[81] Y. Osada, H. Okuzaki, H. Hori, *Nature* **1992**, *355*, 242–244.
[82] Y. Ma, Y. Zhang, B. Wu, W. Sun, Z. Li, J. Sun, *Angew. Chem. Int. Ed.* **2011**, *50*, 6254–6257.
[83] G. H. Kwon, J. Y. Park, J. Y. Kim, M. L. Frisk, D. J. Beebe, S. H. Lee, *Small* **2008**, *4*, 2148–2153.
[84] E. Smela, *Adv. Mater.* **2003**, *15*, 481–494.
[85] a) E. Smela, O. Inganas, I. Lundstrom, *Science* **1995**, *268*, 1735–1738; b) E. W. H. Jager, E. Smela, O. Inganas, *Science* **2000**, *290*, 1540–1545.
[86] A. W. Feinberg, A. Feigel, S. S. Shevkoplyas, S. Sheehy, G. M. Whitesides, K. K. Parker, *Science* **2007**, *317*, 1366–1370.
[87] J. C. Nawroth, H. Lee, A. W. Feinberg, C. M. Ripplinger, M. L. McCain, A. Grosberg, J. O. Dabiri, K. K. Parker, *Nat. Biotechnol.* **2012**, *30*, 792–797.
[88] V. Chan, K. Park, M. B. Collens, H. Kong, T. A. Saif, R. Bashir, *Sci. Rep.* **2012**, *2*, 857.
[89] a) S. Yang, K. Khare, P. C. Lin, *Adv. Funct. Mater.* **2010**, *20*, 2550–2564; b) T. R. Hendricks, W. Wang, I. Lee, *Soft Matter* **2010**, *6*, 3701–3706; c) X. Chen, J. Yin, *Soft Matter* **2010**, *6*, 5667–5680; d) A. Schweikart, N. Pazos-Perez, R. A. Alvarez-Puebla, A. Fery, *Soft Matter* **2011**, *7*, 4093–4100; e) A. Schweikart, A. Fery, *Microchim. Acta* **2009**, *165*, 249–263; f) J. Genzer, J. Groenewold, *Soft Matter* **2006**, *2*, 310–323.
[90] G. Huang, Y. Mei, *Adv. Mater.* **2012**, *24*, 2517–2546.
[91] a) D. H. Gracias, *Curr. Opin. Chem. Eng.* **2013**, *2*, 112–119; b) C. L. Randall, E. Gultepe, D. H. Gracias, *Trends Biotechnol.* **2012**, *30*, 138–146.
[92] T. S. Kelby, M. Wang, W. T. S. Huck, *Adv. Funct. Mater.* **2011**, *21*, 652–657.
[93] A. Azam, K. E. Laflin, M. Jamal, R. Fernandes, D. H. Gracias, *Biomed. Microdevices* **2011**, *13*, 51–58.
[94] a) K. Kumar, B. Nandan, V. Luchnikov, F. Simon, A. Vyalikh, U. Scheler, M. Stamm, *Chem. Mat.* **2009**, *21*, 4282–4287; b) K. Kumar, V. Luchnikov, B. Nandan, V. Senkovskyy, M. Stamm, *Eur. Polym. J.* **2008**, *44*, 4115–4121; c) N. Bassik, B. T. Abebe, K. E. Laflin, D. H. Gracias, *Polymer* **2010**, *51*, 6093–6098; d) S. Singamaneni, M. E. McConney, V. V. Tsukruk, *Adv. Mater.* **2010**, *22*, 1263–1268; e) S. Singamaneni, M. E. McConney, V. V. Tsukruk, *ACS Nano* **2010**, *4*, 2327–2337; f) T. S. Shim, S.-H. Kim, C.-J. Heo, H. C. Jeon, S.-M. Yang, *Angew. Chem. Int. Ed.* **2012**, *51*, 1420–1423.
[95] T. Tanaka, M. Okayama, Y. Kitayama, Y. Kagawa, M. Okubo, *Langmuir* **2010**, *26*, 7843–7847.
[96] a) T. G. Leong, B. R. Benson, E. K. Call, D. H. Gracias, *Small* **2008**, *4*, 1605–1609; b) T. G. Leong, C. L. Randall, B. R. Benson, A. M. Zarafshar, D. H. Gracias, *Lab Chip* **2008**, *8*, 1621–1624; c) T. G. Leong, C. L. Randall, B. R. Benson, N. Bassik, G. M. Stern, D. H. Gracias, *Proc. Natl. Acad. Sci. USA* **2009**, *106*, 703–708.
[97] E. W. H. Jager, O. Inganas, I. Lundstrom, *Science* **2000**, *288*, 2335–2338.
[98] a) X. Zhang, C. L. Pint, M. H. Lee, B. E. Schubert, A. Jamshidi, K. Takei, H. Ko, A. Gillies, R. Bardhan, J. J. Urban, M. Wu, R. Fearing, A. Javey, *Nano Lett.* **2011**, *11*, 3239–3244; b) Y. Liu, J. K. Boyles, J. Genzer, M. D. Dickey, *Soft Matter* **2012**, *8*, 1764–1769; c) J. Ryu, M. D'Amato, X. Cui, K. N. Long, H. J. Qi, M. L. Dunn, *Appl. Phys. Lett.* **2012**, *100*, 161908.
[99] S. Zakharchenko, E. Sperling, L. Ionov, *Biomacromolecules* **2011**, *12*, 2211–2215.
[100] a) K. Kuribayashi-Shigetomi, H. Onoe, S. Takeuchi, in IEEE 25th International Conference, *Micro Electro Mechanical Systems (MEMS),* **2012,** pp. 72–75; b) K. Kuribayashi-Shigetomi, H. Onoe, S. Takeuchi, *Plos One* **2012**, *7*, e51085.
[101] C. L. Randall, Y. V. Kalinin, M. Jamal, A. Shah, D. H. Gracias, *Nanomed. Nanotechnol.* **2011**, *7*, 686–689.
[102] E. Gultepe, J. S. Randhawa, S. Kadam, S. Yamanaka, F. M. Selaru, E. J. Shin, A. N. Kalloo, D. H. Gracias, *Adv. Mater.* **2012**, *25*, 514–519.
[103] a) C. L. Randall, Y. V. Kalinin, M. Jamal, T. Manohar, D. H. Gracias, *Lab Chip* **2011**, *11*, 127–131; b) M. Jamal, N. Bassik, J. H. Cho, C. L. Randall, D. H. Gracias, *Biomaterials* **2010**, *31*, 1683–1690.
[104] a) Y. V. Kalinin, J. S. Randhawa, D. H. Gracias, *Angew. Chem. Int. Ed.* **2011**, *50*, 2549–2553; b) S. Pedron, S. van Lierop, P. Horstman, R. Penterman, D. J. Broer, E. Peeters, *Adv. Funct. Mater.* **2011**, *21*, 1624–1630.
[105] M. Jamal, S. S. Kadam, R. Xiao, F. Jivan, T.-M. Onn, R. Fernandes, T. D. Nguyen, D. H. Gracias, *Adv. Healthcare Mater.* **2013**, 10.1002/adhm.201200458.
[106] B. Yuan, Y. Jin, Y. Sun, D. Wang, J. Sun, Z. Wang, W. Zhang, X. Jiang, *Adv. Mater.* **2012**, *24*, 890–896.
[107] K. Kumar, B. Nandan, P. Formanek, M. Stamm, *J. Mater. Chem.* **2011**, *21*, 10813–10817.
[108] M. Jamal, A. M. Zarafshar, D. H. Gracias, *Nat. Commun.* **2011**, *2*, 527.
[109] V. A. Luchnikov, Y. Saito, L. Tzanis, *Macromol. Rapid Commun.* **2012**, *33*, 1404–1408.
[110] A. Azam, K. Laflin, M. Jamal, R. Fernandes, D. Gracias, *Biomed. Microdevices* **2011**, *13*, 51–58.
[111] B. Y. Ahn, D. Shoji, C. J. Hansen, E. Hong, D. C. Dunand, J. A. Lewis, *Adv. Mater.* **2010**, *22*, 2251–2254.